POST-INSPECTION THERMAL MODELING OF HI-STORM 100 STORAGE MODULES AT DIABLO CANYON POWER PLANT ISFSI

Fuel Cycle Research & Development

Prepared for
U.S. Department of Energy
Used Fuel Disposition Campaign

JM Cuta
HE Adkins
September 30, 2015
FCRD-UFD-2015-000492
PNNL-24771

Reviewed by:

PNNL Project Manager

Signature on file

_____

Brady Hanson

SUMMARY

This report fulfills the M3 milestone M3FT-15PN080100413.

Thermal analysis is being undertaken at Pacific Northwest National Laboratory (PNNL) in support of inspections of selected storage modules at various locations around the United States, as part of the Used Fuel Disposition Campaign of the U.S. Department of Energy, Office of Nuclear Energy (DOE-NE) Fuel Cycle Research and Development. This report documents post-inspection evaluations of temperatures measured in two modules at the Diablo Canyon Power Plant independent spent fuel storage installation (ISFSI), which were inspected in January 2014. These are HI-STORM 100 modules of a site-specific design for storing pressurized water reactor (PWR) 17x17 fuel in MPC-32 (multi-purpose canisters). Pre-inspection predictions of temperatures for these two modules were documented prior to obtaining measured data from the inspection. However, the thermal model developed for the pre-inspection predictions was based on the model developed for the inspection at Hope Creek ISFSI, which has HI-STORM100S-218, Version B modules.

This modeling choice was a "place-holder" to produce pre-inspection predictions, due to the unavailability of site-specific design data for Diablo Canyon ISFSI modules prior to the planned inspection date. Subsequent to the publication of the M4 report documenting the "pre-inspection predictions" for Diablo Canyon, and some time after the inspection had been performed at that site (in January 2014), detailed information on the site-specific design was provided for the thermal modeling work. This information showed that the configuration of the modules at Diablo Canyon is based on the HI-STORM100-SA, which has geometry and design details that differ significantly from the HI-STORM100S-218, Version B geometry used to construct models for the pre-inspection predictions. Therefore, those evaluations are of historical interest only, and are not discussed in this post-inspection report.

The temperature predictions reported in this document were obtained with detailed COBRA-SFS modeling of the HI-STORM100-SA with MPC-32 canister, with site-specific modifications implemented at Diablo Canyon. Models were developed for the two modules, with their individual fuel loading patterns and total decay heat loads. Thermal evaluations were performed with these models, using the following boundary conditions and assumptions.

- Individual assembly and total decay heat loadings for each canister (identified as MPC-123 and MPC-170), were based on at-loading values provided by Pacific Gas and Electric Company (PG&E). These values were "aged" to time of inspection (originally scheduled for December 2013, actually performed in January 2014) using ORIGEN modeling.
    - Special Note: there is an inherent conservatism of unquantified magnitude – informally estimated as up to approximately 20% – in the utility-supplied values for at-loading assembly decay heat values.
- Axial decay heat distribution is based on a bounding generic profile for PWR fuel; no information was provided on axial burnup profiles specific to Diablo Canyon fuel assemblies.
- Axial location of beginning of fuel was assumed to be the same as WE 17x17 OFA fuel, due to unavailability of specific data for the WE 17x17 STD and WE 17x17 Vantage 5 fuel assemblies actually stored in MPC-123 and MPC-170.

- Ambient conditions of still air at 70°F (21°C) and 80°F (27°C), based on the range of measured ambient air temperatures obtained at the site when the inspection was being performed (January 14-16, 2014).
    - Wind conditions at the Diablo Canyon site are unquantified, due to unavailability of site meteorological data, but anecdotal reports from on-site observers at the time of the inspection indicate that there was no appreciable wind over the entire three days, during the intervals of inspection activities.

All COBRA-SFS model calculations are for steady-state conditions, on the assumption that the surfaces of the module that are accessible for temperature measurements during the inspection will tend to follow typical diurnal ambient temperature changes relatively closely. Transient evaluations are beyond the scope of this effort, and would be of little use in this particular case, as there is insufficient data to evaluate measured surface temperature changes over time at the site, and complete data was not recorded on the full range of local ambient conditions (i.e., wind speed as well as ambient temperature) during the time period of the inspection. No measurements are available on wind conditions at the ISFSI during the time surface temperature measurements were obtained, but on-site observers report essentially still air for all three days of the inspection. The actual conditions of the inspection were therefore reasonably congruent with the assumption of still air used in the thermal analyses.

Measured temperatures were obtained on the side surfaces and top lid surfaces of the canisters in the two modules that were inspected. The side surface temperatures were obtained on a single axial line, determined by the location of the outlet vent that was used to insert the measurement tool into the annulus between the canister and the overpack. However, information on the orientation of the canister within the overpack, relative to the orientation of the basket structure within the canister is not tracked in the canister loading process. Therefore, it is not possible to determine the orientation of the fuel within the canister, with respect to the location of the line of measured temperatures.

This was not an issue in the inspections at the Hope Creek IFSI, since the basket within an MPC-68[1] canister effectively fills the entire cavity cross-section, with relatively uniform gaps near the wall. The canisters stored in the Hope Creek ISFSI, therefore, were predicted to have an essentially uniform circumferential temperature distribution at any given axial location along the length of the canister. Therefore, the actual geometric location of the line of temperature measurements was not important, for the purpose of comparing model results to measured temperature data. For the MPC-32 canisters at Diablo Canyon, however, the design of the basket results in large non-uniform gaps between the periphery of the basket and the cavity wall. This is illustrated by the MPC-32 cross-section in Figure S-1. This internal structural geometry results in a non-uniform circumferential temperature distribution at any given location along the axial length of the fuel within the canister, as illustrated in Figure S-2.

[1] This MPC number should not be confused with the MPC numbers used to identify the storage modules inspected at the Diablo Canyon or Hope Creek ISFSIs. MPC-68 is Holtec's designation for the particular canister type that is in use at the Hope Creek ISFSI, and holds 68 BWR fuel assemblies. MPC-32 is Holtec's designation for the particular canister type in use at the Diablo Canyon ISFSI, which is designed to hold 32 PWR fuel assemblies.

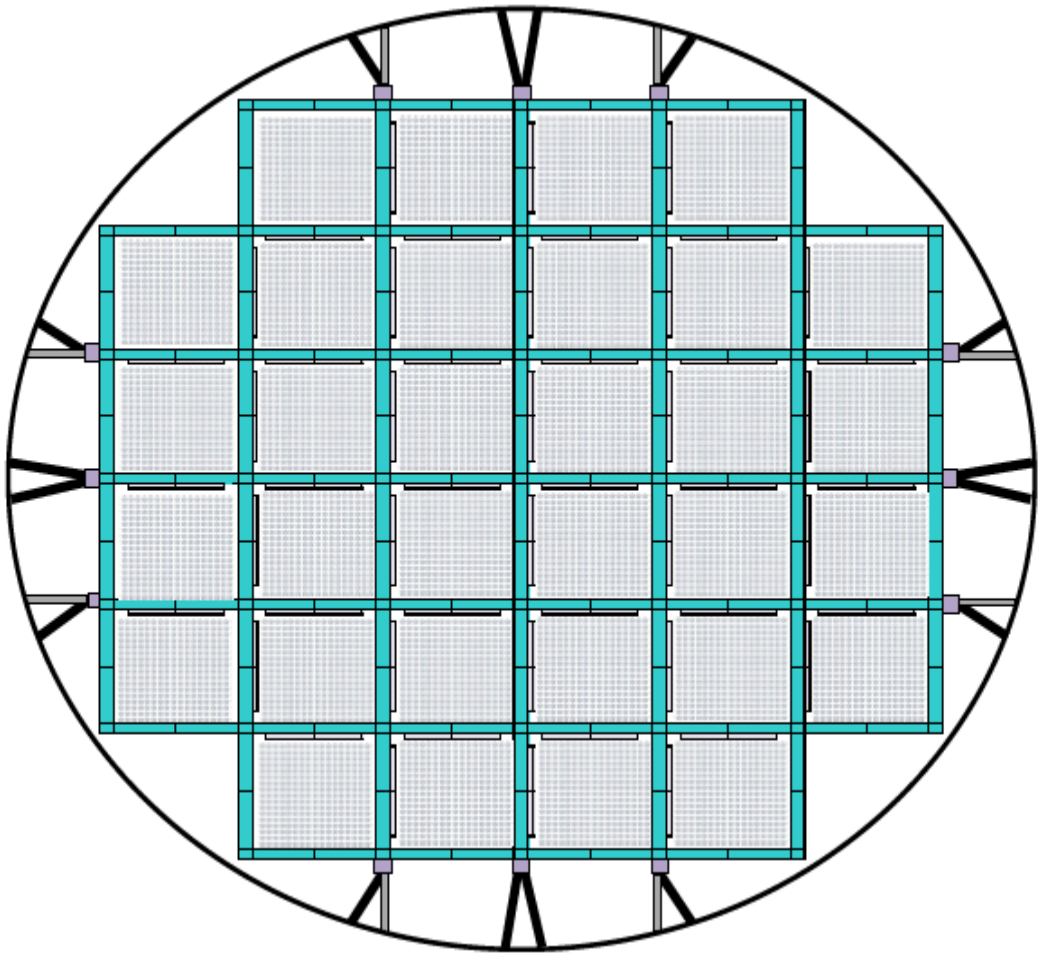

Figure S-1. Diagram of 3-D COBRA-SFS Model of MPC-32 Canister in Thermal Model of Diablo Canyon Storage Module (NOTE: diagram not to scale; node thicknesses greatly exaggerated for clarity)

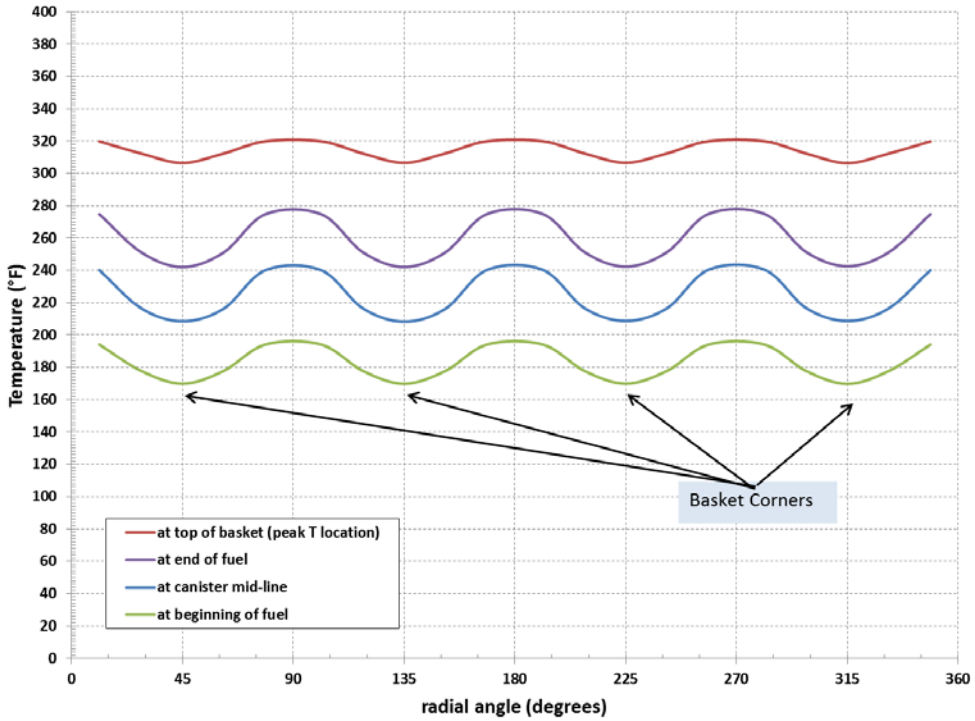

Figure S-2. Circumferential Temperature Distributions on MPC Outer Shell: Module #318

Because of this circumferential variation in predicted temperatures, the comparisons between COBRA-SFS modeling results and the measured temperatures on the canister side surface are shown along axial lines at the maximum predicted temperature at a given circumferential location (i.e., over the face of the basket), and at the minimum predicted temperature (i.e., over the corner of the basket). Figure S-3 shows this approach to comparison between the model results and the measured temperatures obtained on the side surface of MPC-170. Figure S-4 shows a similar comparison from the inspection of MPC-123.

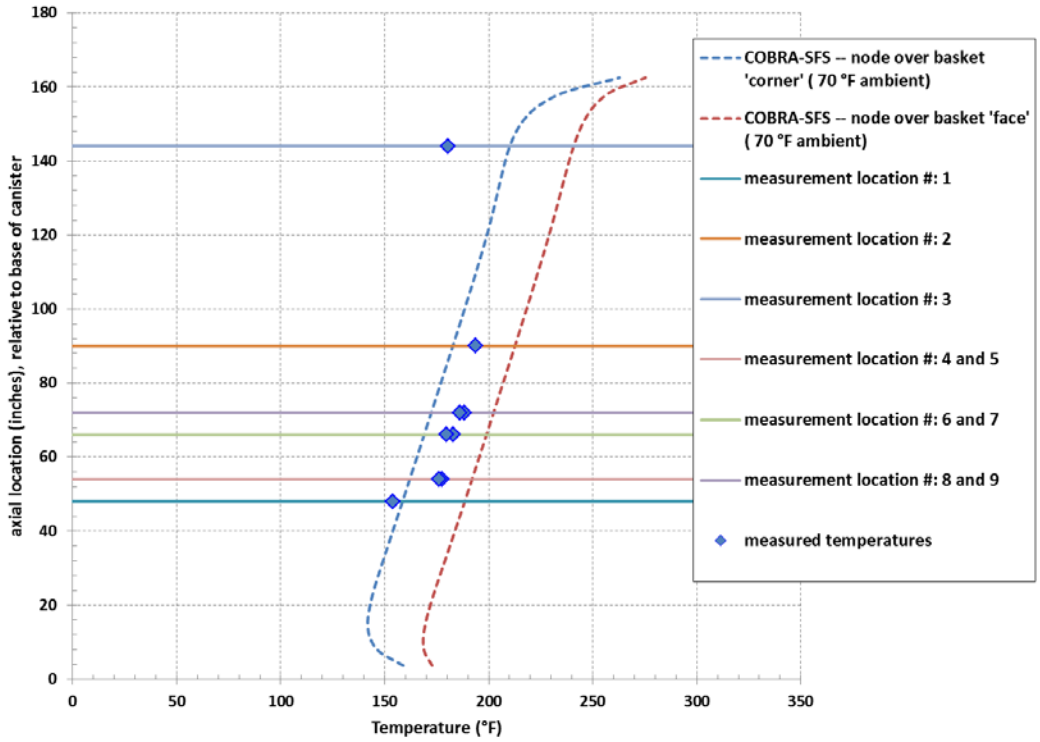

Figure S-3. Comparison of Axial Profiles from Thermal Modeling Results (at 70°F Ambient) to Measured Side Surface Temperatures on MPC-170

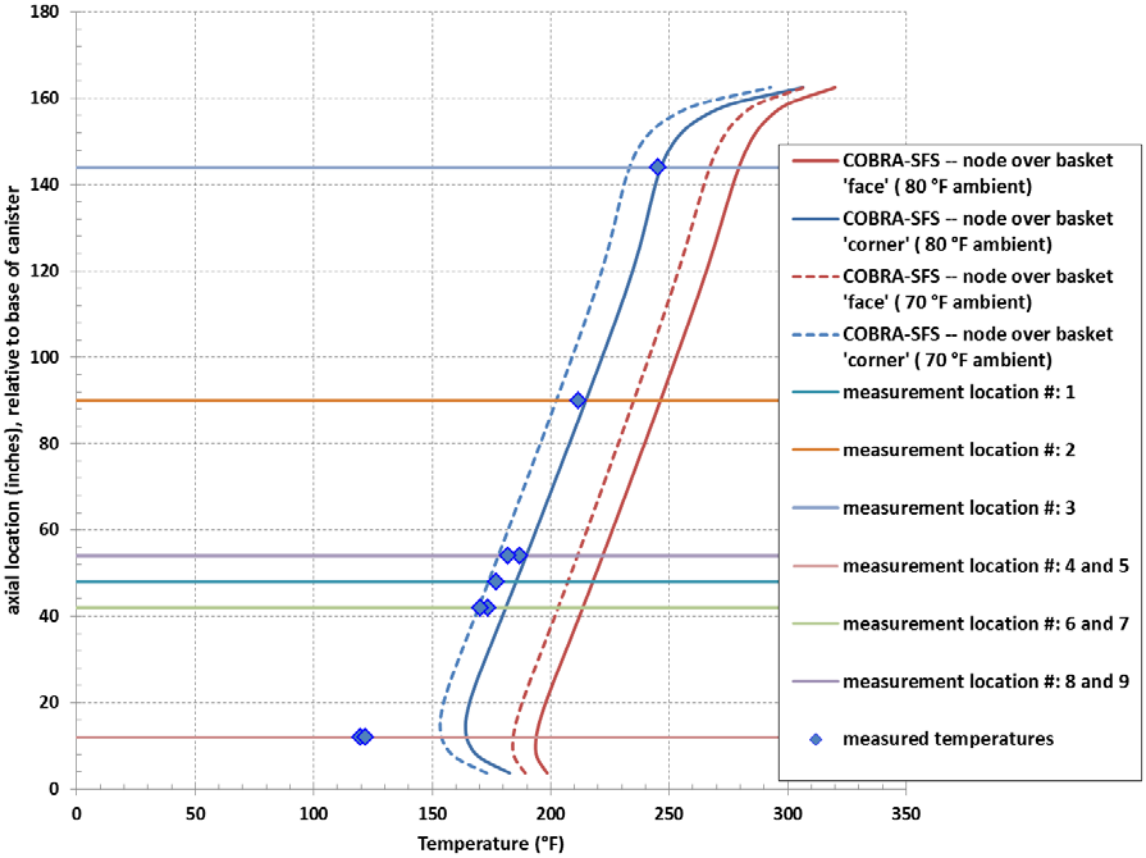

Figure S-4. Comparison of Axial Profiles from Thermal Modeling Results (at 70°F Ambient and 80°F Ambient) to Measured Side Surface Temperatures on MPC-123

These results show that the measured temperatures fall between the maximum and minimum temperature profiles predicted on the side surfaces of each canister. Given that the actual line of measurement, relative to the face and corner locations of the interior basket, is not known, this comparison shows very good agreement between the model and the measured temperature data. Some of the measured temperatures near the near the ends of the canister side, however, fall well below the predicted profiles at these locations. One possible explanation for this difference is that the actual axial decay heat profile of the fuel within the canister differs significantly from the assumed bounding axial decay heat at locations near the ends of the active fuel length.

Temperature measurements were obtained on the top lid surface of the inspected modules (MPC-170 and MPC-123) at only at two locations, and these locations are near the outer rim of the canister lid. Measurements were not obtained along the diameter of the lid surface, or near the lid center. Two points near the rim, without information on the radial temperature profile across the lid, is not sufficient to produce a meaningful comparison to COBRA-SFS model predictions for the lid surface. The COBRA-SFS model uses a relatively simple 1-D representation of the canister and overpack lid region, and a meaningful comparison would require sufficient radial temperature data to obtain an estimate of the average lid surface temperature. Therefore, the top lid surface measurements have been omitted from the comparisons with model results.

ACKNOWLEDGEMENTS

Special thanks are owed to Keith Waldrop of EPRI and Lawrence Pulley of PG&E, for supplying assembly loading data for the canisters selected as candidates for the inspection.

ACRONYMS AND ABBREVIATIONS

BWR	Boiling Water Reactor
CFD	computational fluid dynamics
DOE	U.S. Department of Energy
DOE-NE	U. S. Department of Energy Office of Nuclear Energy
DSC	dry shielded canister
EPRI	Electric Power Research Institute
FEA	finite element analysis
ISFSI	independent spent fuel storage installation
MPC	multi-purpose canister
NCDC	National Climatic Data Center
NOAA	National Oceanic and Atmospheric Administration
ORNL	Oak Ridge National Laboratory
PG&E	Pacific Gas and Electric Company (owner/operator of Diablo Canyon power plant and ISFSI)
PNNL	Pacific Northwest National Laboratory
PWR	Pressurized Water Reactor
UFDC	Used Fuel Disposition Campaign
WE	Westinghouse

CONTENTS

FIGURES

TABLES

POST-INSPECTION THERMAL MODELING OF HI-STORM 100 STORAGE MODULES AT DIABLO CANYON POWER PLANT ISFSI

1.0 INTRODUCTION

As part of the Used Fuel Disposition Campaign of the U.S. Department of Energy, Office of Nuclear Energy (DOE-NE) Fuel Cycle Research and Development, a consortium of national laboratories[2] and industry[3] are performing inspections and temperature measurements of selected storage modules at various locations around the United States. In June 2012, inspections were performed on two horizontal storage modules in the Calvert Cliffs Nuclear Power Station's Independent Spent Fuel Storage Installation (ISFSI). Inspections were performed in November 2013 at the Hope Creek Nuclear Generating Station ISFSI, and in January 2014 at the Diablo Canyon Nuclear Power Station ISFSI. Thermal analysis in support of these inspections has been undertaken at Pacific Northwest National Laboratory (PNNL).

Pre-inspection and post-inspection evaluations have been performed for the modules examined at Calvert Cliffs (Suffield et al. 2012) and Hope Creek (Cuta and Adkins 2013; Cuta and Adkins 2015). Pre-inspection predictions of temperatures for the selected modules in the ISFSI at Hope Creek were published prior to the actual inspection of the modules at Hope Creek, in November 2013. Post-inspection evaluations, published in 2015, compare the pre-inspection predictions with the measured data from the Hope Creek inspection. No additional information on the modules or fuel stored in them was provided after the inspection, and the pre-inspection calculations spanned the full range of ambient temperatures at the site at the time of the inspection. Therefore, for the Hope Creek inspection, there was no basis for making revised calculations with post-inspection thermal modeling.

Pre-inspection evaluations were performed for modules inspected at the Diablo Canyon Power Plant ISFSI (Cuta and Adkins, 2014), on the assumption that the models developed for the module overpack at Hope Creek (representing the HI-STORM 100S-218 Version B system) would be reasonably representative of the modules at Diablo Canyon. It was assumed that the only significant difference would be in the multi-purpose canister (MPC) configuration, which is the MPC-32 at Diablo Canyon, and MPC-68 at Hope Creek. Information provided after the inspection (which occurred in January 2014) showed that this assumption was overly optimistic. There are significant differences in the site-specific HI-STORM 100 SA design at Diablo Canyon, compared to the modules at Hope Creek, such that the predictions in the pre-inspection report for Diablo Canyon are of historical interest only. The current report on post-inspection modeling for the Diablo Canyon ISFSI presents only results obtained with models revised to

[2] Pacific Northwest National Laboratory, Oak Ridge National Laboratory, Sandia National Laboratories, and Idaho National Laboratory

[3] Electric Power Research Institute, TN/AREVA, Holtec International, PSEG Nuclear LLC (owner of Hope Creek Nuclear Generating Station), Constellation Energy (Owner of Calvert Cliffs Nuclear Power Station), and Pacific Gas and Electric Corporation (owner of Diablo Canyon Power Plant).

conform to the late-provided site-specific information on the configuration of the HI-STORM100 SA modules and MPC-32 canisters at Diablo Canyon.

The importance of specific design features notwithstanding, the basic feature of a HI-STORM 100 system, regardless of the specific configuration, consists of a helium-pressurized stainless steel canister (MPC) that is loaded into a vertical steel-lined concrete overpack. The spent fuel is contained within the sealed canister, and the basket internal design varies with the type of fuel to be stored, with three main configurations available for Pressurized Water Reactor (PWR) fuel assemblies and two for Boiling Water Reactor (BWR) fuel assemblies. Thermal models have been developed for the modules that were inspected at Diablo Canyon, using COBRA-SFS (Michener et al. 1995), a code developed by PNNL for thermal-hydraulic analyses of multi-assembly spent fuel storage and transportation systems.

The COBRA-SFS code uses a finite-difference subchannel analysis approach for predicting flow and temperature distributions in spent fuel storage systems and fuel assemblies under forced and natural circulation flow conditions. It is applicable to both steady-state and transient conditions in single-phase gas-cooled spent fuel packages with radiation, convection, and conduction heat transfer. The code has been validated in blind pretest calculations using test data from spent fuel packages loaded with actual spent fuel assemblies as well as electrically heated single-assembly tests (Creer et al. 1987, Rector et al. 1986, Lombardo et al. 1986).

The data obtained in these on-site inspections provide an opportunity to develop structural and thermal models that can yield realistic predictions for actual storage systems, in contrast to conservative and bounding design-basis calculations. The analytical approach used in this study does not include many of the conservatisms and bounding assumptions normally used in design-basis and safety-basis calculations for spent fuel storage systems.

The storage modules selected for the site inspection at the Diablo Canyon Power Plant's ISFSI are designated as HI-STORM #318 and #516. The canisters stored within these two modules are designated MPC-123 and MPC-170. The fuel stored within these MPCs is designated by loading campaign number and order of canister loading; 02-02 for the fuel assemblies in MPC-123 and 03-05 for the fuel assemblies in MPC-170. The measured data obtained in the inspection at Diablo Canyon is reported in terms of results from MPC-123 and MPC-170, and this is the primary identifier used in the thermal modeling results. However, the identifier from the fuel loading is also used, as this is the identifier used in the transmission of fuel decay heat and loading patterns. When these secondary identifiers are used in this report, the MPC identifier is also noted, to avoid potential confusion. Images of typical dry casks in place at the Diablo Canyon site can be viewed on the public internet site FLICKR, maintained and supported by Yahoo.com, at

http://www.flickr.com/photos/nrcgov/6871626011/in/photostream/

These images are from the U.S. Nuclear Regulatory Commission, a member of FLICKR since 2011, and are part of the photostream labeled "NRCgov" on this site, which currently runs to 1,393 images.

Figure 1-1 contains a generic not-to-scale diagram illustrating the structure of the site-specific HI-STORM100 SA modules at the Diablo Canyon ISFSI. The main feature to note in this diagram is the relatively large gap between the top of the canister and the inner surface of the overpack lid. This is due to the non-standard (short) canister size in use at Diablo Canyon, due to constraints imposed by the geometry of their fuel handling facility. A line drawing of a typical HI-STORM100 module is shown in Figure 1-2. The 100-SA site-specific design at Diablo Canyon differs in some details from this image, particularly in the lid configuration. In addition, the modules at the Diablo Canyon ISFSI do not contain the shim channels on the inner surface of the overpack wall.

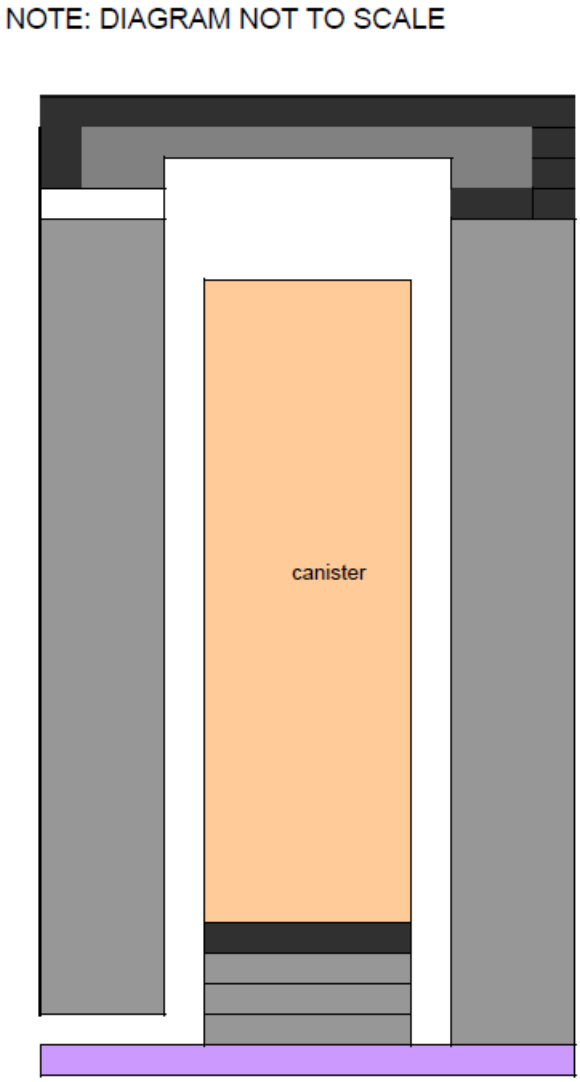

Figure 1-1. Generic Diagram Showing Main Features of HI-STORM100 SA Module Design

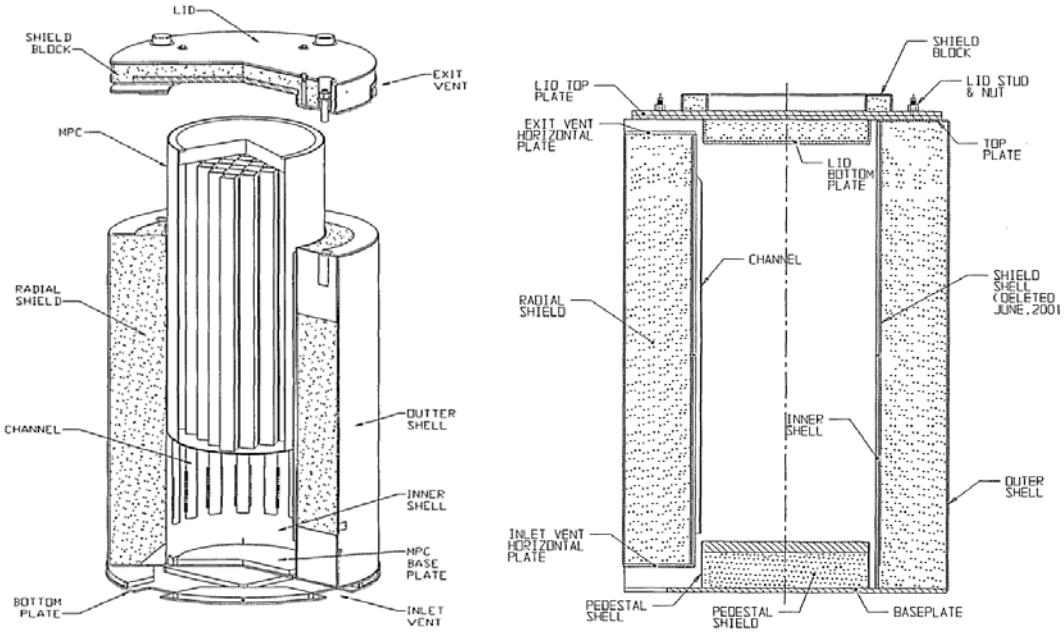

Figure 1-2. Typical HI-STORM 100S Vertical Storage Module (Image courtesy of Holtec International; reprinted with permission)

The two modules selected for inspection in the Diablo Canyon ISFSI are essentially identical, except for the multi-purpose canister (MPC) contents, which vary significantly in total decay heat load and loading pattern. Thermal models have been developed and evaluations performed for both modules, for comparison to measured data obtained at the time of the inspection (January 2014).

The COBRA-SFS model geometry for the site-specific HI-STORM100SA with MPC-32 canisters is described in detail in Section 2. This section also presents the boundary conditions and modeling assumptions for the evaluations of temperatures in the modules that were inspected at the Diablo Canyon ISFSI. Section 3 presents post-inspection predictions of component temperatures and temperature distributions within the modules, for a range of ambient conditions consistent with measured temperatures on site at the time of the inspection. Section 4 presents the measured temperature data obtained during the inspection, and compares the measurements to the thermal modeling results presented in Section 3. Conclusions and recommendations are summarized in Section 5.

2.0 COBRA-SFS MODEL DESCRIPTION

The HI-STORM100 system is a vertical storage module design developed by Holtec International, and consists of an MPC inserted into a steel-lined concrete overpack (Holtec 2010). The general design of the overpack is similar for all configurations of the system, such that the main site-specific character of a particular installation is the design of the canister stored within the overpack. At the Diablo Canyon ISFSI, the canister design is the MPC-32, which is for PWR fuel, and stores up to 32 PWR fuel assemblies. The canisters in the storage modules to be inspected in the Diablo Canyon ISFSI are designated 02-02 and 03-05, in reference to campaign and canister number at the time of loading of spent fuel into the canisters. The first number in the designation refers to the dry storage loading campaign number, and the second number identifies the cask in that campaign sequence. Canisters in campaign 01 were loaded in June-August 2009; canisters in campaign 02 were loaded in May-July 2010, and canisters in campaign 03 were loaded in Jan-Feb 2012. The canisters loaded in each campaign were also assigned specific identifying numbers, MPC-xxx. The specific overpack modules these two canisters are loaded into are designated HI-STORM #318 (for 02-02, loaded into MPC-123) and HI-STORM #516 (for 03-05, loaded into MPC-170).

A COBRA-SFS model for a vertical storage system such as the HI-STORM 100, of whatever specific configuration, consists of three major pieces; the canister, the air flow channel that allows external ambient air to circulate through the module, and the external overpack surrounding the canister. Information on the site-specific design of the modules at Diablo Canyon was not provided to PNNL before the actual inspection date, due to delays in implementing Non-Disclosure Agreements (NDAs) with the various parties involved. Therefore, for the pre-inspection thermal analysis of the selected modules at the Diablo Canyon ISFSI, the HI-STORM 100 overpack was modeled utilizing the COBRA-SFS model developed for the Hope Creek inspections (Cuta and Adkins, 2013). Subsequent to the actual inspection date (in January 2014), additional site-specific information on the overpack module and canister design at the Diablo Canyon ISFSI was supplied for the thermal modeling work. This information showed significant differences between the 100S-218 Version B and the site-specific 100A configuration at Diablo Canyon. This required significant revision to the thermal models for the two modules inspected at the Diablo Canyon site, and as a result, there are no useful pre-inspection results to compare with the measured data. The models described in this section are based on post-inspection information on the site-specific designs.

The general structure of the model of the site-specific HI-STORM 100SA storage system used in the Diablo Canyon ISFSI is illustrated in Figure 2-1. The detailed three-dimensional nodalization of the fuel assemblies, basket, canister, and overpack walls extends only over the axial length of the basket within the MPC. This highly detailed portion of the model represents the region of radial heat transfer from the fuel rods to the ambient environment. The axial length of this region is defined by the length of the basket, which in this case is 17.3 cm (6.81 inches) short of the total axial length of the canister internal cavity. Axial heat transfer out the top and bottom of the system is represented with a simpler, one-dimensional thermal resistance network, consisting of the upper and lower plenum regions.

Diagrams illustrating the model representation of the entire system are shown in Figures 2-2 and 2-3. For clarity, the canister and overpack portions of the model are shown separately. Figure 2-

2 shows a cross-section diagram of the canister portion of the model, including the fuel rods, basket plates (with neutron poison plates), basket support structure, and canister shell. Different colors are used for different components, for clarity in the complex mesh. This diagram is not to scale, since in a scaled diagram of the mesh, fine details such as the neutron poison plates are difficult to discern. In addition, the detailed rod-and-subchannel arrays within the basket cells are shown with the rod spacing greatly exaggerated, so that the subchannels are visible.

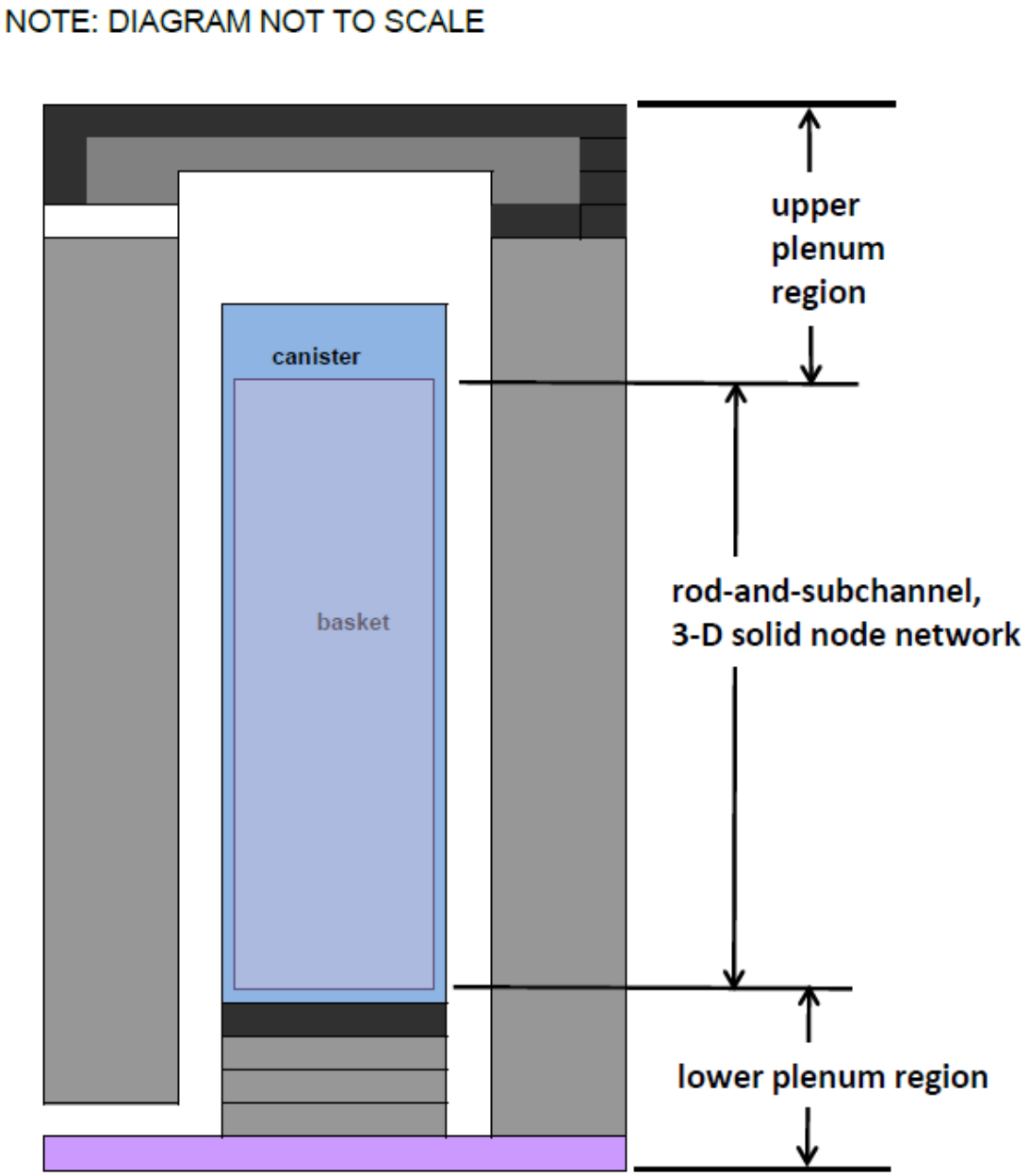

Figure 2-1. Diagram of Modeling Regions in COBRA-SFS Model of site-specific HI-STORM 100SA Vertical Storage System at Diablo Canyon (NOTE: diagram is not to scale)

Figure 2-3 shows a cross-section diagram of the portion of the model representing the overpack. The pre-inspection modeling, based on typical HI-STORM100 configurations (including the

modules at Hope Creek), assumed the presence of channel shims on the inner wall of the overpack liner. The actual configuration of the modules at the Diablo Canyon ISFSI omits these shims, and they are not included in the thermal model for the post-inspection evaluations. The geometry of both modules inspected is assumed to be identical, and therefore the images in Figures 2-2 and 2-3 illustrate the thermal models for both modules. The only significant difference in the models for the two modules is in the assembly loading pattern, which is unique for each module. The representation of the decay heat in the fuel assemblies in the COBRA-SFS modeling is discussed in detail in Section 2.1.

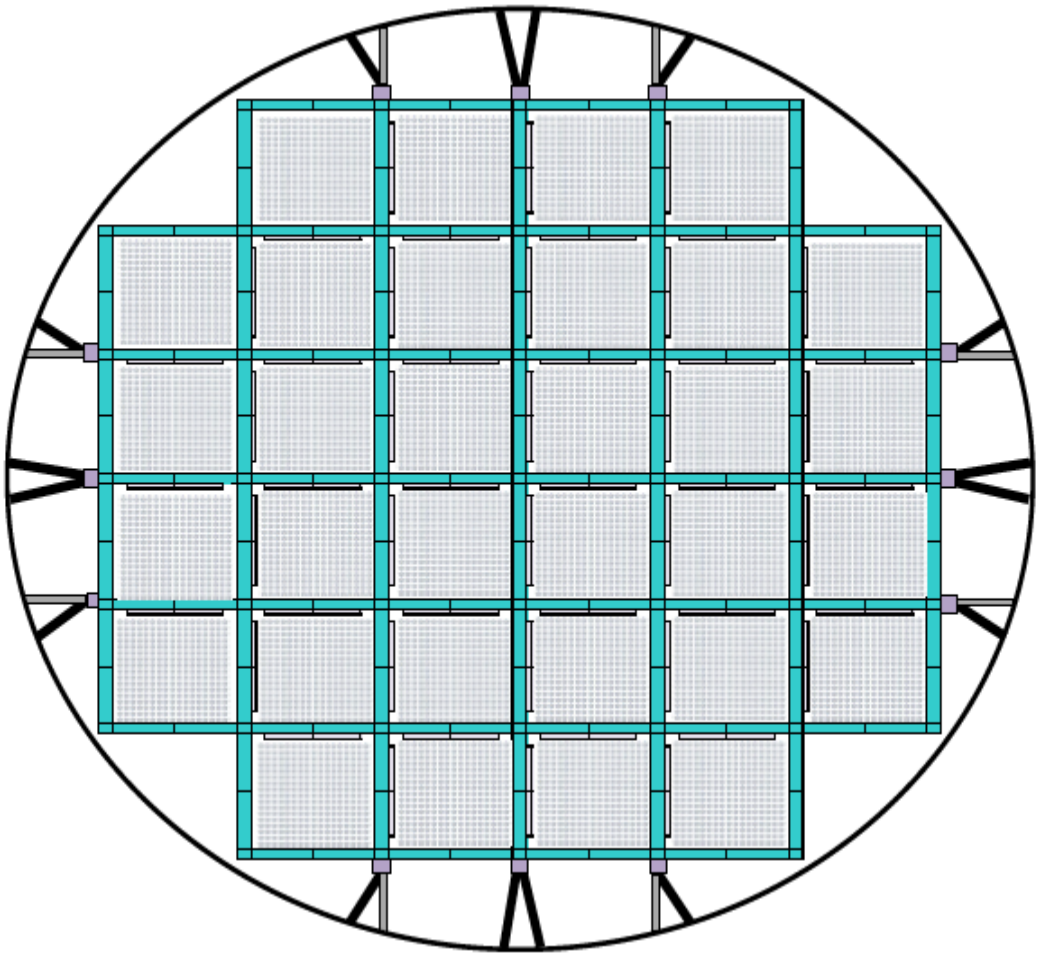

Figure 2-2. Diagram of 3-D COBRA-SFS Model of MPC-32 Canister in Thermal Model of Diablo Canyon Storage Module (NOTE: diagram not to scale; node thicknesses greatly exaggerated for clarity)

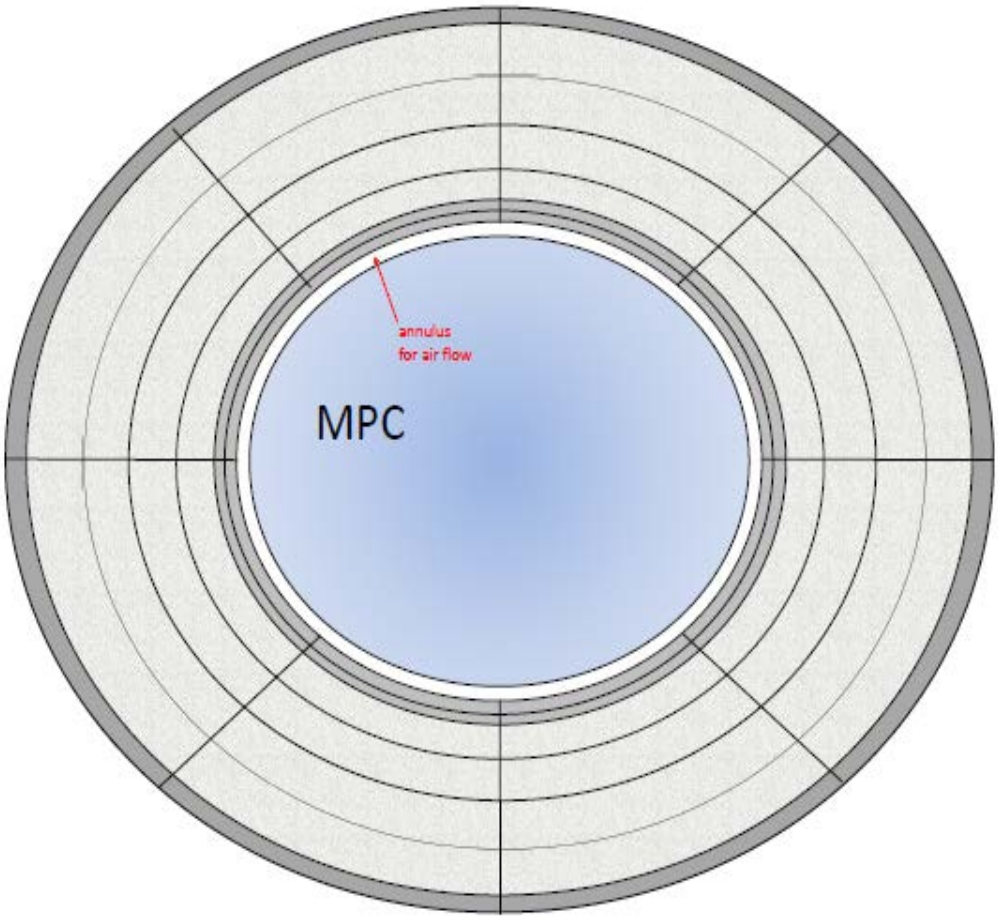

Figure 2-3. Cross-section of COBRA-SFS Model of Diablo Canyon Site-Specific Overpack for HI-STORM100SA (NOTE: diagram is not to scale. Air annulus width and steel thicknesses are greatly exaggerated for clarity.)

The detailed model of the canister and internals (including the fuel assemblies) shown in Figure 2-2 has the typical mesh resolution generally used for the basket structure in COBRA-SFS models of spent fuel storage systems. Finer mesh resolution can be specified, if needed, but comparison with temperature measurements from single-assembly and multi-assembly experiments, including testing of storage systems with spent fuel loaded in the basket (Lombardo et al. 1986; Rector et al. 1986; Creer et al. 1987) has shown that this meshing is sufficient for resolution of temperature gradients typical of spent fuel storage systems. The mesh includes the basket plates, poison plates, and basket support structures, including the shims on these structures that are used to ensure firm contact between the basket frame and canister inner shell.

The thermal network approach used in COBRA-SFS allows direct representation of thin plates and the contact resistance due to small gaps between adjacent components. In typical models for computational fluid dynamics (CFD) and finite element analysis (FEA) codes, structures consisting of adjacent thin plates (such as the basket plates, poison plates, and poison plate sheathing) are modeled as a single material with homogenized properties. The approach used in COBRA-SFS of modeling the individual thin plates and the appropriate contact resistances

between them allows more detailed resolution of temperature distributions in such structures, using a comparatively smaller mesh.

As shown in Figure 2-2, the main feature of the COBRA-SFS model of the canister is the representation of the flow field within the fuel assemblies in the basket, and the flow paths external to the basket that allow recirculation due to natural convection within the canister. Within the individual basket cells, the fuel assembly and flow field is represented with a detailed subchannel model. This representation of the fuel assembly allows for much more accurate resolution of the local rod temperatures, compared to the typical approach used in CFD and FEA models, in which the fuel assembly region is represented as a homogeneous block with internal heat generation, or as a porous medium. The detailed rod-and-subchannel model allows the code to calculate individual fuel rod cladding temperatures, accounting for heat transfer by conduction, convection, and thermal radiation, and permits detailed modeling of material parameters, such as fuel cladding emissivity and surface conditions.

The detailed rod-and-subchannel array within a basket cell is illustrated in Figure 2-4 for a single WE 17x17 assembly. The fuel stored in the canisters of the Diablo Canyon ISFSI consist of two different configurations of WE 17x17 fuel; WE 17x17 Standard (STD) and WE 17x17 Vantage 5. These fuel designs have essentially the same physical geometry, but differ slightly in fuel rod diameter. The detailed COBRA-SFS model accounts for this geometry difference in the rod-and-subchannel model array in each of the basket cells of the canister. The two canisters evaluated each have a unique arrangement of the two different fuel types, as discussed in Section 2.1.

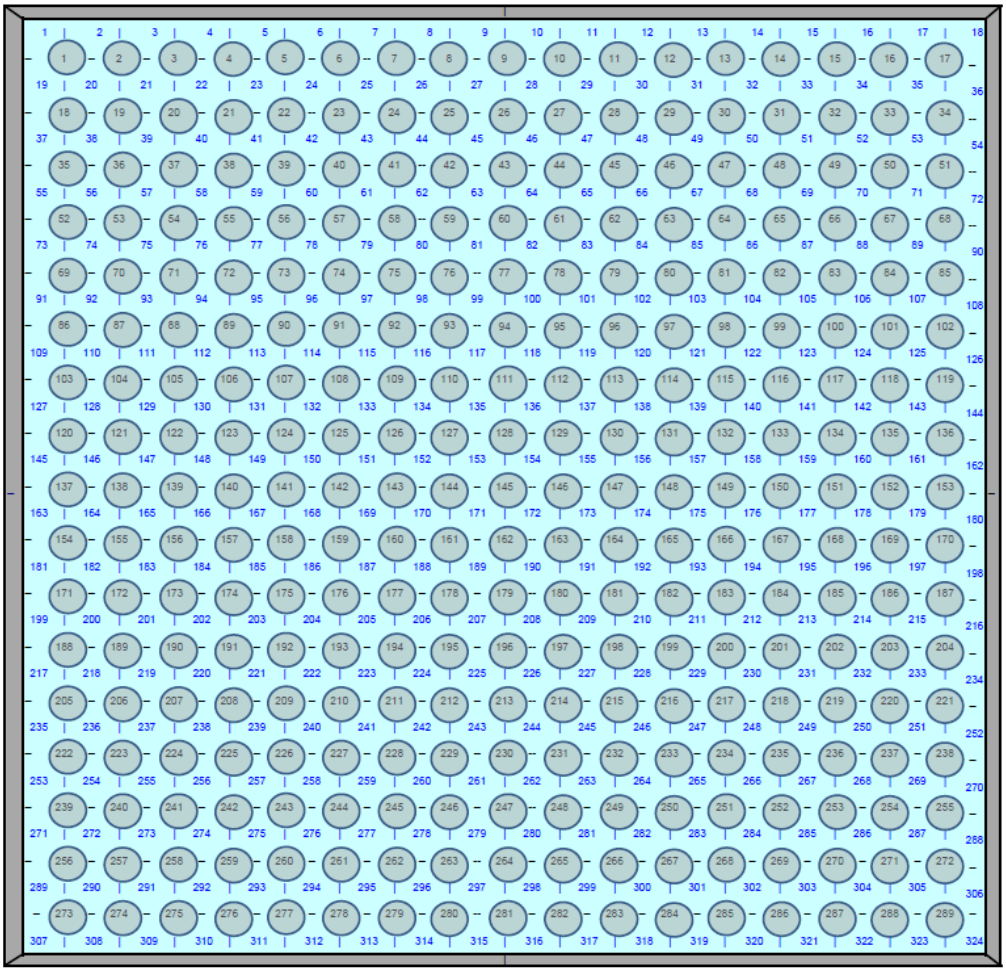

Figure 2-4. Rod-and-subchannel Array Diagram for COBRA-SFS Model of WE 17x17 Fuel Assembly within Basket Cell (Note: diagram is not to scale; rod spacing is greatly exaggerated for clarity.)

For convection heat transfer, the fluid channels within the canister are thermally connected to the fuel rods and to the surrounding solid conduction nodes representing the basket by means of a user-specified heat transfer correlation. Based on validation of the COBRA-SFS code with experimental data from vertical test systems and canisters loaded with actual spent fuel, convection heat transfer in the fuel rod array is represented with the venerable Dittus-Boelter heat transfer correlation for turbulent flow,

$$Nu = 0.023(Re^{0.8})(Pr^{0.4})$$

where Nu = Nusselt number
Re = Reynolds number, based on subchannel hydraulic diameter
Pr = Prandtl number for the backfill gas

For laminar flow conditions, a Nusselt number of 3.66 has been verified as applicable to spent fuel rod arrays. The local heat transfer coefficient is defined as the maximum of the values calculated from the laminar and turbulent correlations specified by user input. Figure 2-5

illustrates the convenient mathematical behavior of these correlations as a function of Reynolds number.

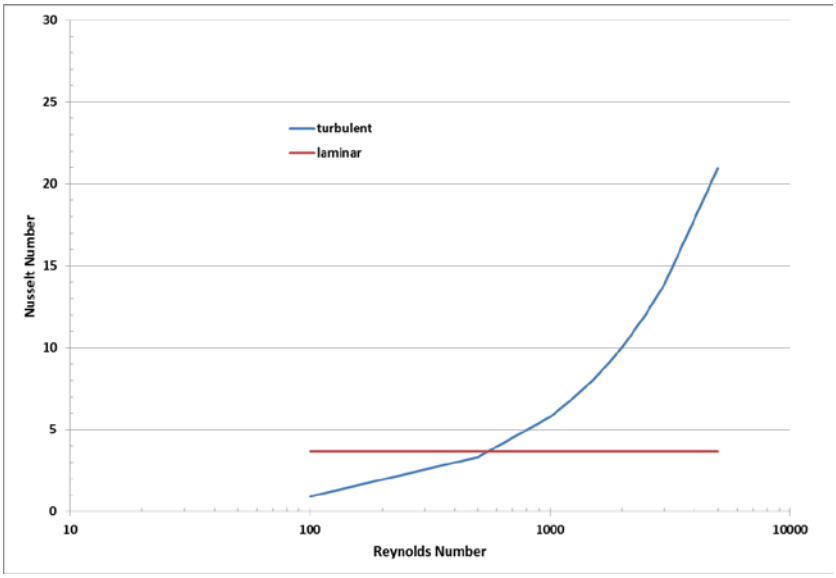

Figure 2-5. Laminar and Turbulent Formulations for Nusselt Number

In addition to convection heat transfer, the fluid energy equation includes conduction through the fluid (helium gas) in the subchannels, and the gas is assumed transparent to thermal radiation. Thermal radiation within the basket is calculated using 2-dimensional (planar cross-section) grey-body view factors for the rod array and surrounding solid conduction nodes of the basket wall. The view factors are calculated for the specific assembly and basket cell geometry using the auxiliary code RADGEN, which is part of the COBRA-SFS package. Thermal radiation across the geometrically simpler flow channels between the basket and the canister shell are determined in COBRA-SFS directly from user-input black body view factors, calculated using the Hottel crossed-string correlation methodology. Based on the specified surface emissivity of the nodes of the surfaces of a given flow region, the code calculates the grey-body view factors for thermal radiation exchange.

The annulus between the canister and the overpack is represented in the COBRA-SFS model with four flow channels, each representing a quadrant of the annulus region cross-section. Since the site-specific configuration of the overpack for the modules in the Diablo Canyon ISFSI does not include the shim channels spaced around the inner shell of the storage cavity (typically 16, spaced 22.5° apart around the annulus), azimuthal resolution of the annulus is necessary only to capture the configuration of the inlet and outlet vents. It is assumed that the canister is positioned symmetrically within the overpack cavity, and the annulus channel width is modeled as uniform around the circumference. The fact that the inspection tool used to obtain the measurements on the side surface of the MPC actually managed to fit down the annulus is a reasonable confirmation of the validity of this assumption. Air flow in the fluid channels representing the annulus is calculated using a pressure drop boundary condition based on the height of the system and the specified ambient air temperature. Momentum losses are determined using a friction factor correlation and form drag losses due to the orificing effects of the inlet and exit structures above and below the annulus.

Thermal connections between the annulus flow channels and the solid conduction nodes of the MPC shell and overpack inner shell are defined in the COBRA-SFS model for conduction and thermal radiation heat transfer. Convection heat transfer in the air annulus is treated as a forced convection flow, driven by the imbalance between the hydrostatic pressure drop within the annulus and that of the ambient air external to the overpack (Sparrow and Azevedo 1985). The Dittus-Boelter correlation has been shown to be an appropriate heat transfer model for prediction of heat transfer in a vertical storage module (Creer et al., 1987). The air flow in the annulus is expected to be turbulent for normal conditions of storage, but the COBRA-SFS input also includes a lower bound of Nu = 7.44 (derived[4] from Sparrow et al., 1961), which represents laminar flow conditions in a vertical stack. As illustrated in Figure 2-5, the code uses the mathematical behavior of the correlations to automatically select the appropriate flow regime by taking the maximum of the values obtained with the laminar and turbulent formulations for the local flow conditions.

2.1 Fuel Assembly Decay Heat Modeling

The spent fuel stored at the Diablo Canyon ISFSI consists of WE 17x17 assemblies in two slightly different configurations, designated STD and Vantage 5, as noted above in the discussion of fuel assembly geometry modeling with COBRA-SFS. The significant difference between the two designs is the diameter of the active fuel rods, which is slightly smaller in the Vantage 5 fuel. Both configurations have nominally 289 pin positions within the array, with 264 active fuel rods. Information provided by PGE[5] included the individual assembly decay heat loads at the time of loading into an MPC, cooling time as of time of loading, initial enrichment, assembly burnup, and assembly load maps for the canisters in dry storage at the ISFSI, including all modules being considered for inspection.

The methodology used by PGE to determine the individual assembly decay heat values at loading is not specifically referenced, but has been informally identified as a conservative evaluation based on ORIGEN calculations. The decay heat values at the time of the planned inspections were estimated from the "at loading" decay heat values by performing calculations with the Used Nuclear Fuel Storage, Transportation, Disposal Analysis Resources and Data system (UNF-ST&DARDS) (Peterson et al., 2013). These calculations obtained decay heat values in these fuel assemblies as of December 2013, the originally scheduled timeframe of the inspections at the Diablo Canyon ISFSI.

The total canister decay heat loadings for the two modules inspected are summarized in Table 2-1. The decay heat values calculated for all assemblies within the individual canisters are listed in Table 2-2. (The basket location of an assembly is identified by row number and column letter, using the convention illustrated in the diagram in Figure 2-6.) These tables include the values reported for the time of loading and values calculated for the time of the inspection, originally scheduled for December 2013. The time of actual inspection, in January 2014, is close enough to December 2013 for the change in decay heat over that one-month time interval to be well within the uncertainty of the modeling.

[4] The mean value in the reference is Nu=7.86. The value of 7.44 represents the lower bound on the ±5% uncertainty in the data.

[5] Provided in spreadsheet 'Info on Assemblies In ISFSI.xls', sheet 'All Campaigns – reviewed', transmitted as an attachment to e-mail from Keith Waldrop of EPRI (sent Thursday 4/25/2013 12:05pm PDT).

Table 2-1. Total Decay Heat Loading per Module

Module	ORIGEN decay heat (kW)	
	at loading	at inspection
#318 MPC 123 (02-02)	20.10 (5/17/2010)	17.05
# 516 MPC 170 (03-05)	15.39 (2/13/2012)	13.87

Table 2-2. Assembly Decay Heat Loadings for Modules Inspected at Diablo Canyon ISFSI

Basket cell location	Assembly decay heat (W)			
	at time of loading		December 2013 (inspection timeframe)	
	Module #318 MPC 123 (02-02)	Module # 516 MPC 170 (03-05)	Module #318 MPC 123 (02-02)	Module # 516 MPC 170 (03-05)
B-1	520.4	407.41	467.0	372.07
C-1	529.6	380.34	451.7	349.80
D-1	544.9	378.31	481.7	347.51
E-1	553.9	379.2	491.8	345.48
A-2	566.1	302.61	501.9	275.87
B-2	567.1	410.42	503.8	374.82
C-2	580.3	618.6	513.7	552.54
D-2	777.6	620.62	602.9	554.10
E-2	568.1	416.48	502.6	381.50
F-2	520.6	361.13	457.1	331.61
A-3	550.9	409.42	488.8	375.16
B-3	834.2	614.56	641.7	549.27
C-3	855.8	663.16	659.5	560.65
D-3	801.3	679.86	621.5	604.70
E-3	752.5	620.64	649.1	552.91
F-3	535.2	362.14	452.9	333.27
A-4	540.8	374.27	479.6	344.24
B-4	773.2	617.61	618.3	551.57
C-4	808.4	654.81	626.4	553.64
D-4	633.5	680.86	544.2	608.18
E-4	778.5	626.71	649.8	559.98
F-4	547.9	378.32	485.7	348.15
A-5	524.6	401.36	463.8	367.68
B-5	578.2	410.43	513.4	374.98
C-5	795.1	616.61	617.1	550.60
D-5	756.6	635.77	652.6	567.78
E-5	572.2	434.28	508.1	404.24
F-5	558	356.09	495.2	328.89
B-6	563	380.21	499.1	350.87
C-6	548.9	379.21	486.6	348.69

D-6	538.8	407.41	476.0	375.67
E-6	524.5	406.39	447.7	372.59

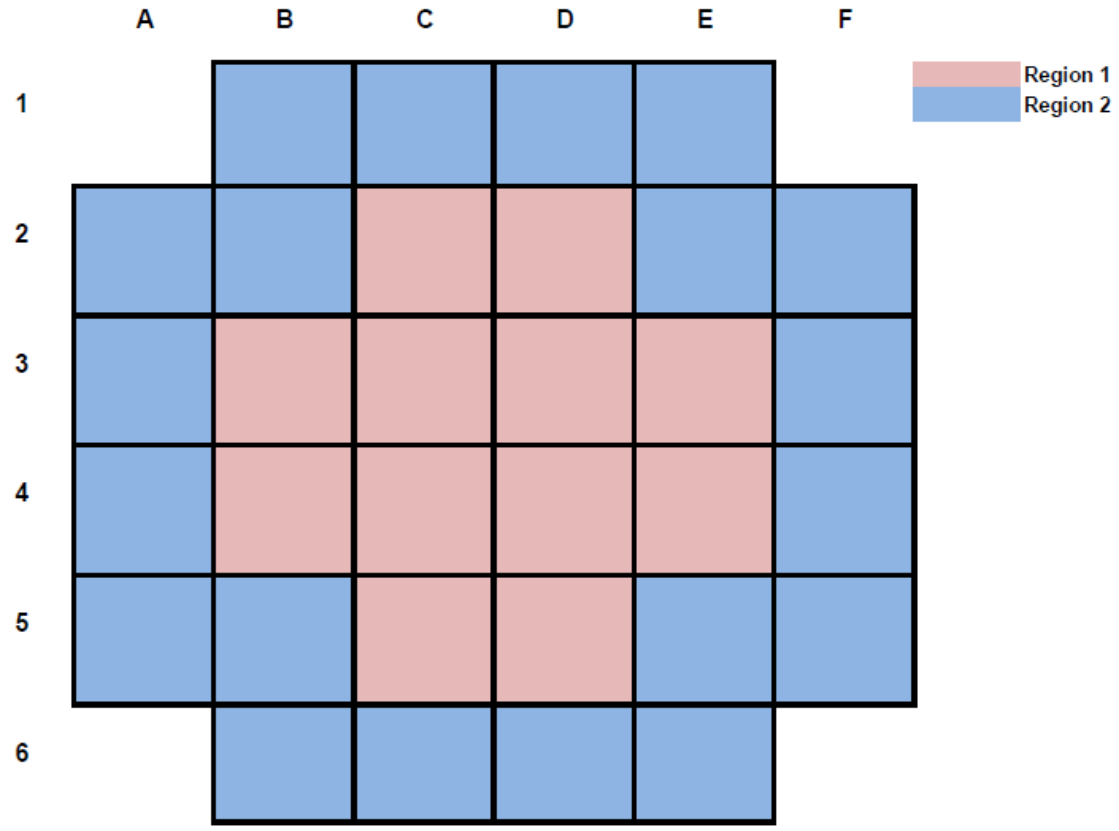

Figure 2-6. Diagram Illustrating Basket Cell Location Convention

The fuel loading pattern within the canister basket, while nominally uniform over the 32 assemblies, in fact is not the same for all assemblies, as shown by the per assembly decay heat values in Table 2-2. In addition, the arrangement of the assemblies within the basket results in some asymmetry in the radial distribution of decay heat loading over the basket cross-section. The distribution of the decay heat load in MPC-123 (02-02) and MPC-170 (03-05) places colder fuel assemblies in the basket “corners”, for radiation self-shielding. This is illustrated in Figures 2-7 through 2-10, with plots of the decay heat values (from ORIGEN calculations for December 2013) for the assemblies within the basket. (Refer to Figure 2-6 for basket row/column cell numbering convention.)

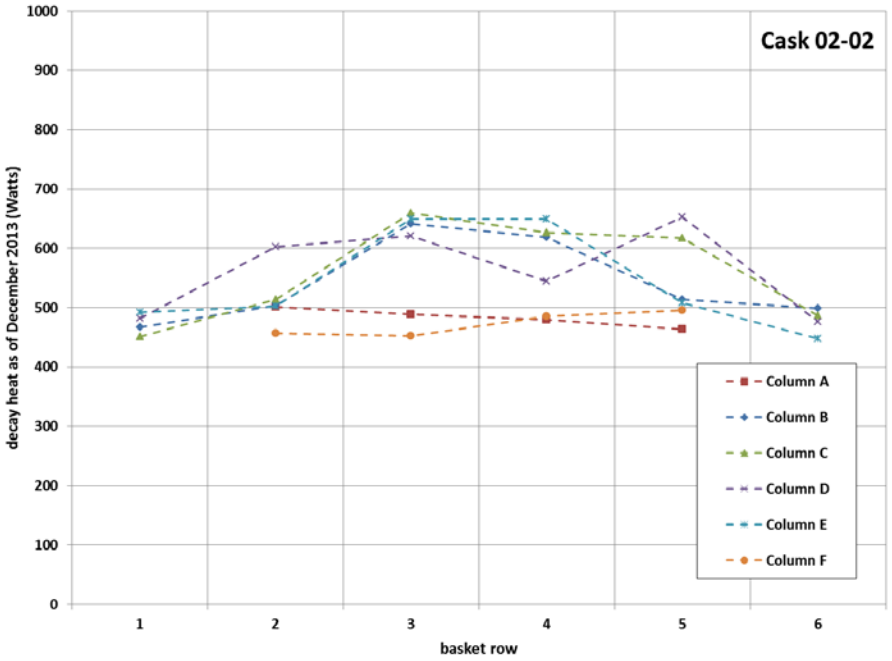

Figure 2-7. Assembly Decay Heat Distribution in MPC-123 (02-02)

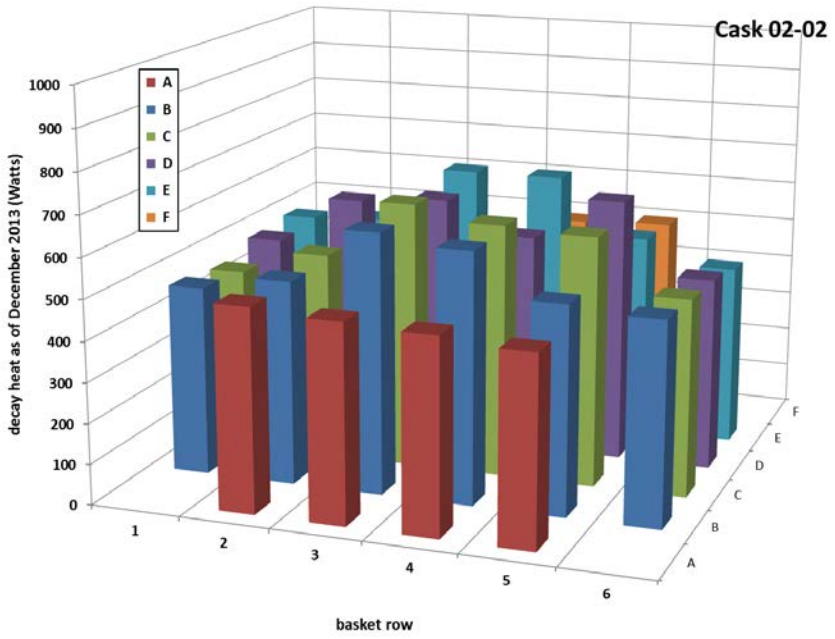

Figure 2-8. 3-D Illustration of Assembly Decay Heat Distribution in MPC-123 (02-02)

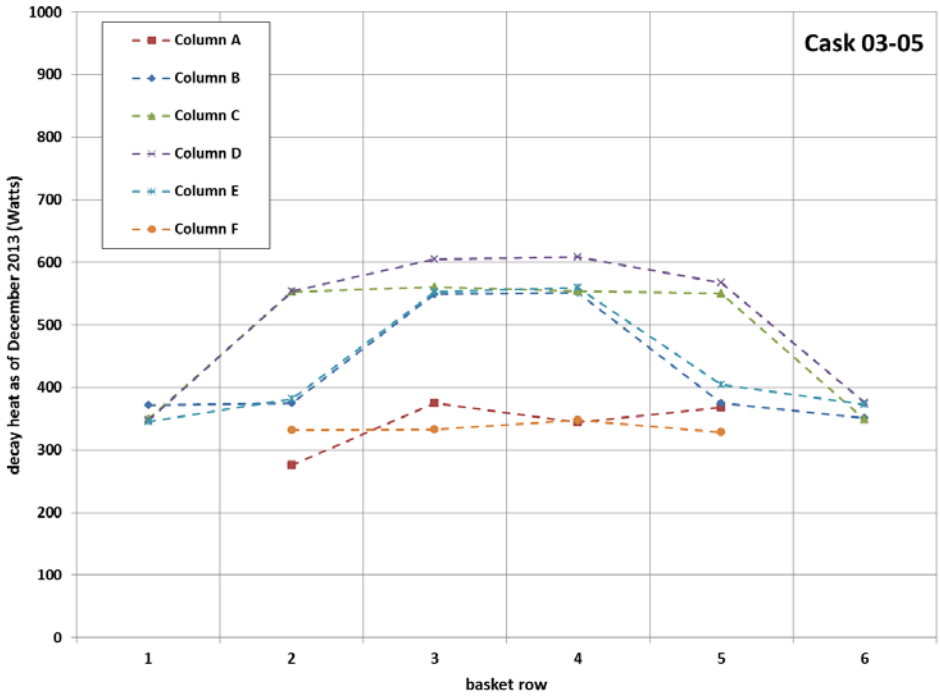

Figure 2-9. Assembly Decay Heat Distribution in MPC-170 (03-05)

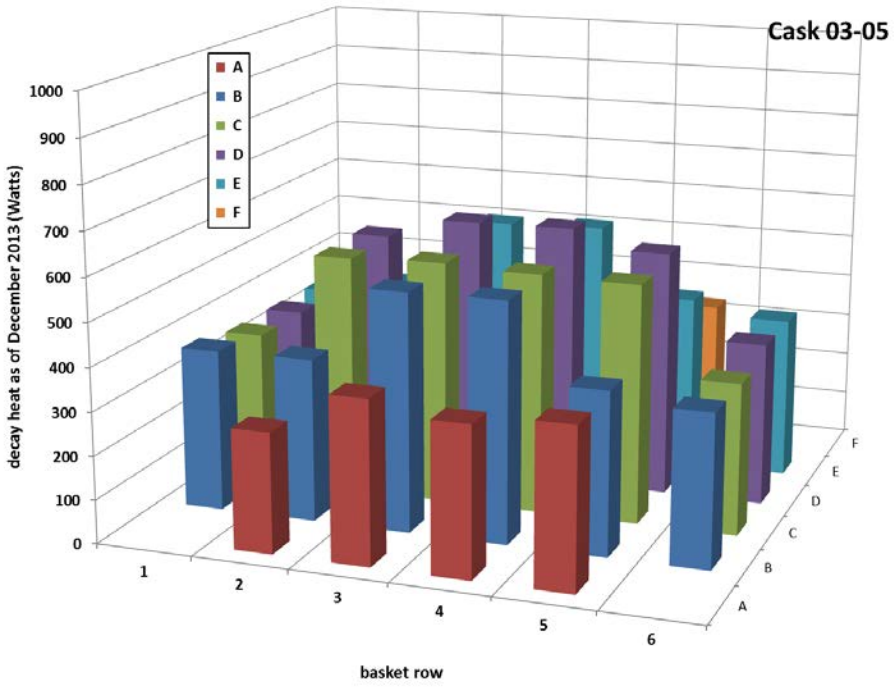

Figure 2-10. 3-D Illustration of Assembly Decay Heat Distribution in MPC-170 (03-05)

The line graphs in Figures 2-7 and 2-9 show the numerical values summarized in Table 2-2 for the two canisters. The column charts provide a more visual illustration of the non-uniform distribution of assembly decay heat values, and show the reduced heat load in the basket corners. Table 2-3 summarizes the maximum, minimum, and average assembly decay heat values for the assemblies in these two canisters. (Refer to Figure 2-6 for location convention.)

Table 2-3. Summary of Decay Heat Variation from Basket Center to Periphery (for December 2013 Calculated Assembly Decay Heat Values)

	peak assembly		**coldest assembly**		**Region 1 average assembly decay heat (Watts)**	**Region 2 average assembly decay heat (Watts)**
Module	**(Watts)**	**location**	**(Watts)**	**location**		
#318 (02-02) MPC 123	660	C-3 (Region 1)	448	B-1 (Region 2)	616	483
#516 (03-05) MPC 170	608	D-4 (Region 1)	276	A-2 (Region 2)	564	355

The axial decay heat distribution for the WE 17x17 fuel within the canisters was modeled with a generic profile for PWR fuel, since axial burnup distributions for the fuel were not included in the fuel data package. This profile, shown in Figure 2-11, is a bounding profile determined for low burnup PWR spent fuel (DOE 1998). More accurate information on the axial decay heat profile would result in more accurate predictions of peak component temperatures within the canister. Because the profile for spent fuel is relatively flat, the uncertainty in peak temperature predictions due to this approximation is probably rather small. Near the ends of the fuel region, however, the profile is expected to drop to near zero over a relatively short distance. This gradient strongly influences the temperature profile near the ends of the fuel rods, and consequently near the ends of the canister. This generic profile, rather than profiles representative of the fuel stored in these modules, is a potential source of uncertainty in the predictions of axial temperature distribution in the thermal modeling.

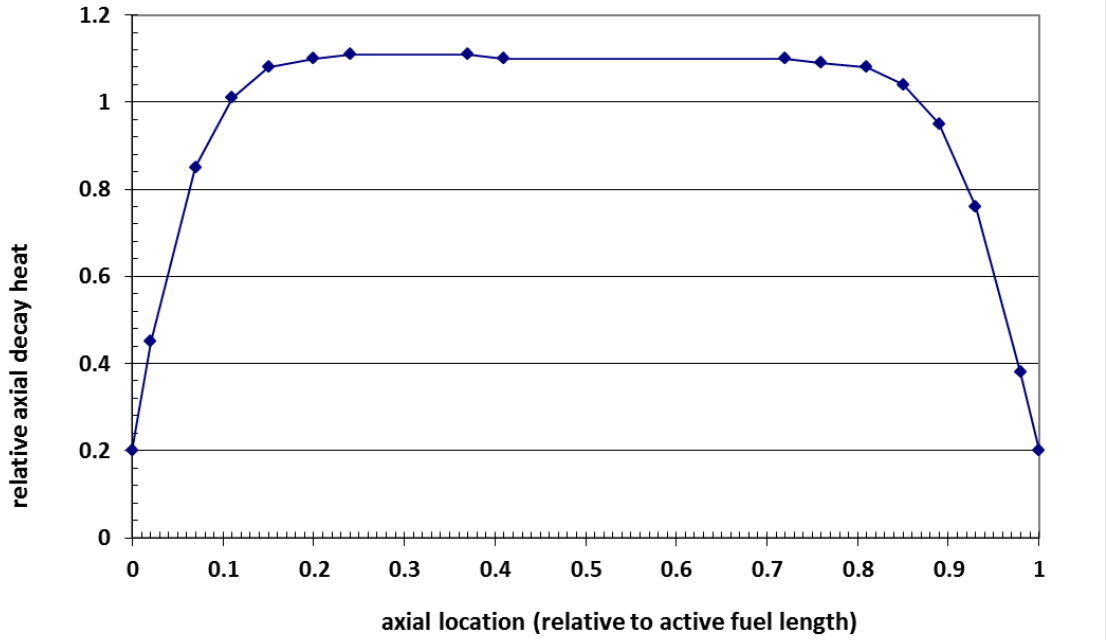

Figure 2-11. Bounding Axial Decay Heat Profile for low burnup PWR Spent Fuel (DOE 1998)

2.2 Ambient Conditions

Ambient conditions at the ISFSI, including air temperature and local surface winds at the time of the inspection, have a significant effect on the temperatures measured on the MPC outer surfaces. No meteorological data has been provided for the Diablo Canyon ISFSI at the time of the inspections (January 14-16, 2014). The only ambient air temperature measurements available are the specific point measurements taken at the time of the surface temperature measurements. Figure 2-12 shows all measured ambient air temperature data obtained during the inspection, consisting of a total of 22 measurements over the thee-day period. These measurements show that the ambient air temperature ranged from 67°F to 80°F (19°C to 27°C), an unusually high temperature for the time of year, even in southern California. However, historical maximum temperatures for the region have reached as high as 85°F (29°C) in January, as recorded by the National Oceanic and Atmospheric Administration (NOAA 2013).

No measurements are available on wind conditions at the ISFSI during the time surface temperature measurements were obtained, but on-site observers report essentially still air for all three days of the inspection. This is also an unusual condition for a sea-side site in canyon-cut topography, but wind and weather answer not to expectations; only to the laws of atmospheric physics. The actual conditions of the inspection, in terms of potential wind effects, are therefore reasonably congruent with the assumption of still air used in the thermal analyses.

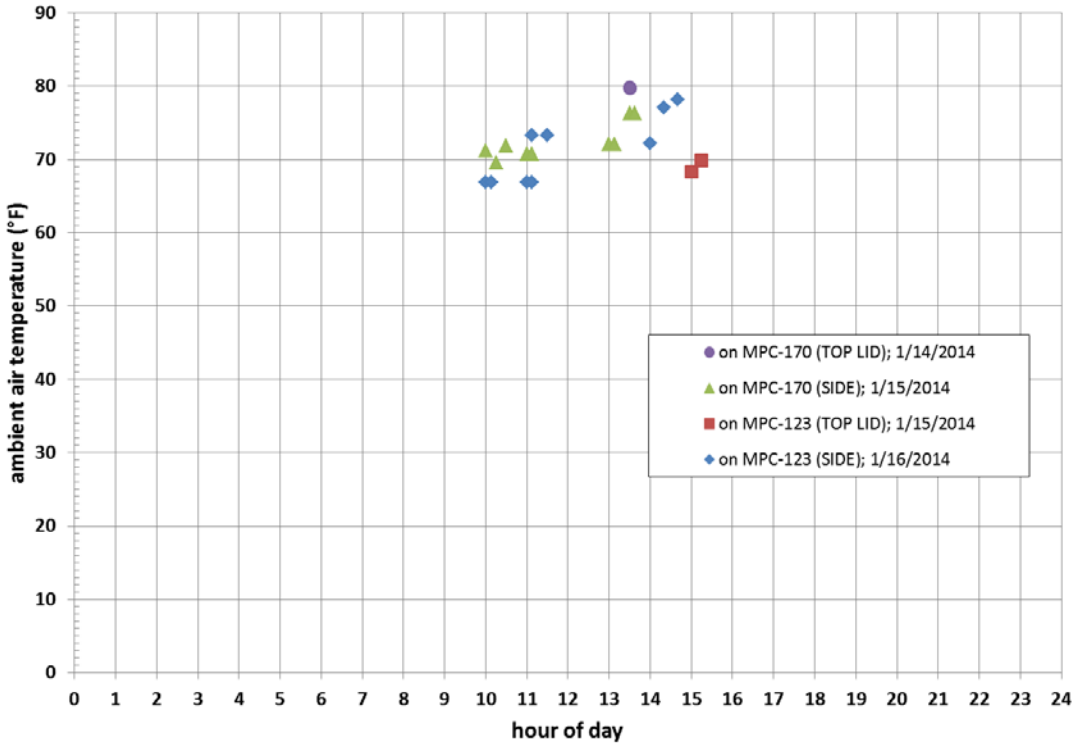

Figure 2-12. Measured Ambient Air Temperatures Obtained in Conjunction with MPC Surface Measurements during Site Inspection at Diablo Canyon ISFSI

The external solar heat load on the modules assumed for these calculations is based on the solar radiation assumptions specified in 10 CFR 71.71 (10 CFR 71). This regulation is specifically for transport conditions, but the specified values are generally used for stationary storage systems, as well. Solar radiation over a 12-hour period is defined in 10 CFR 71.71 as

800 cal/cm^2 (2950 Btu/ft^2) for horizontal surfaces

400 cal/cm^2 (1475 Btu/ft^2) for curved surfaces.

Adjusting for the surface emissivity, which in these evaluations is assumed to be 0.9 for the painted exterior surfaces of the overpack, the above specified values are averaged over a 24-hour period, to obtain the following solar heat flux values for this system:

349 W/m^2 (110.6 Btu/hr-ft^2) on the overpack lid

175 W/m^2 (55.3 Btu/hr-ft^2) on the outer shell.

These values may be conservative for the solar heat load on the modules at the time of the inspection, but in the absence of site-specific information, they will have to do.

3.0 POST-INSPECTION PREDICTIONS OF COMPONENT TEMPERATURES

This section presents a summary of the MPC side surface temperatures predicted with the COBRA-SFS model described in Section 2, for the two modules inspected at the Diablo Canyon ISFSI. (Section 4 presents direct comparisons between the COBRA-SFS predictions and the measured surface temperatures obtained during the inspection.) Two sets of calculations were performed for each module; one for ambient air temperature of 70°F (21°C) and one at 80°F (27°C), to span the range of ambient air temperatures measured at the site during the inspection. Table 3-1 summarizes peak temperatures predicted for components of the canister for the range of ambient conditions at the time of the inspection. Table 3-2 summarizes peak temperatures predicted for components of the overpack for the corresponding cases.

Table 3-1. Peak Component Temperatures, °F (°C), Predicted for Inspected MPCs

Module	ambient air	Fuel cladding	Neutron Poison Plate	Basket plate	Basket periphery	Basket support	Canister inner surface	Canister outer surface
#318 (02-02) MPC 123	70 (21)	409.5 (209.7)	401 (205.3)	401 (205.3)	343 (172.9)	333 (167.4)	307 (153.0)	307 (152.6)
	80 (27)	420.9 (216.1)	415 (212.9)	415 (212.9)	355 (179.7)	346 (174.6)	321 (160.3)	320 (160.0)
#516 (03-05) MPC 170	70 (21)	361.9 (183.3)	356 (180.1)	356 (180.1)	305 (151.7)	297 (147.3)	276 (135.5)	275 (135.2)
	80 (27)	373.3 (189.6)	368 (186.4)	368 (186.4)	315 (157.2)	307 (152.9)	286 (141.2)	286 (140.8)

Table 3-2. Peak Component Temperatures, °F (°C), in Overpack

Module	ambient air	Overpack inner shell	Overpack concrete	Overpack outer shell	Overpack lid inner surface	Overpack lid outer surface
#318 (02-02) MPC 123	70 (21)	162 (72.3)	161 (71.8)	110 (43.4)	161 (71.4)	137 (58.6)
	80 (27)	175 (79.3)	174 (48.8)	120 (48.7)	161 (71.4)	144 (62.4)
#516 (03-05) MPC 170	70 (21)	150 (65.3)	149 (64.9)	109 (42.6)	160 (71.2)	135 (57.4)
	80 (27)	161 (71.7)	160 (71.2)	118 (47.8)	160 (71.2)	144 (62.3)

Axial temperature distributions on the canister shell are presented in Figures 3-1 and 3-2 for the two modules. (Tabular values for all plotted axial profiles are provided in Appendix A.) These plots show temperatures at two different radial locations, to capture the circumferential temperature variation on the canister shell, due to the basket configuration within the MPC-32. The “square peg in a round hole” geometry of the rectilinear basket within the cylindrical canister results in relatively large open regions between the basket corners and the canister shell,

as illustrated in Figure 2-2, in the noding diagram for the COBRA-SFS model of the basket region. The canister shell temperatures are therefore lower in this region, since heat transfer radially is somewhat inhibited by this geometry. The flat "faces" of the basket, in contrast, are physically closer to the wall, and also have direct conduction heat transfer paths to the outer shell through the metal of the basket support structures. As a result, heat is transferred more readily to the canister shell at these locations, and the surface temperature is highest in this region.

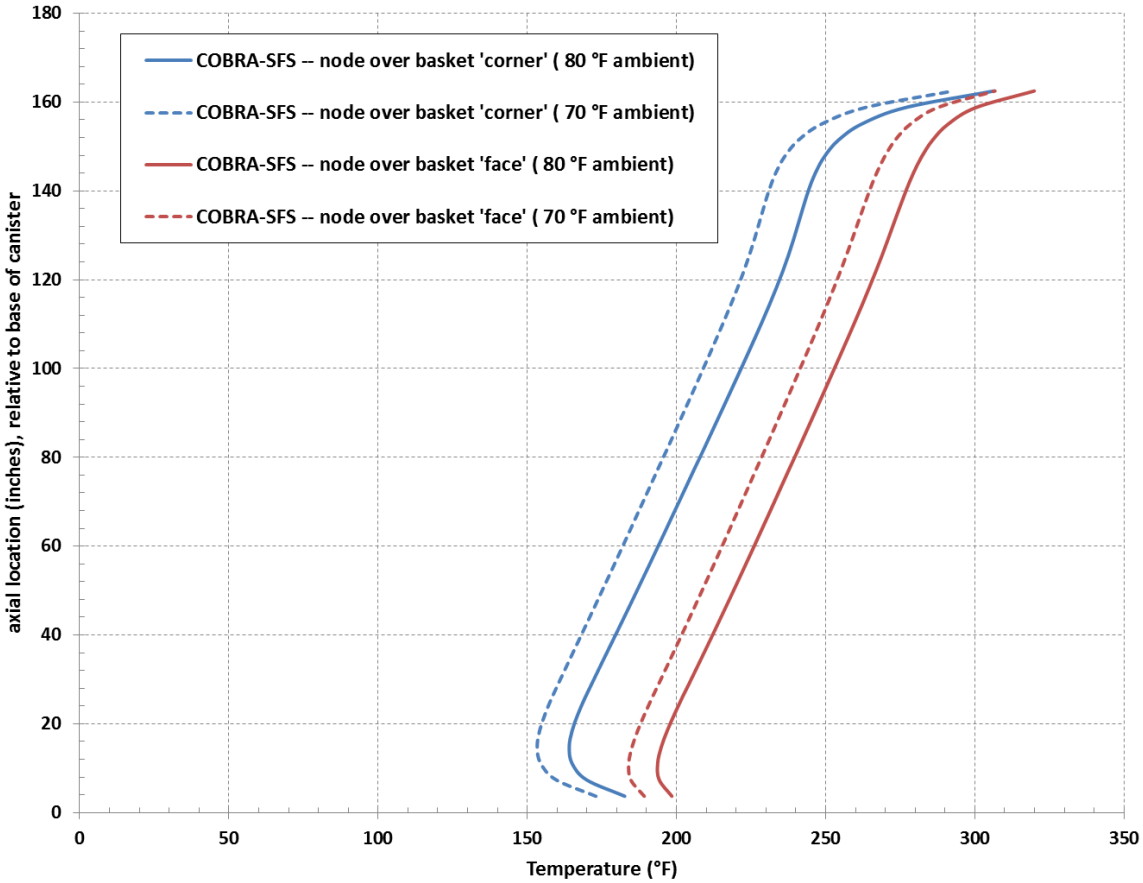

Figure 3-1. Axial Temperature Profiles on MPC Outer Shell: Module #318, MPC-123 (02-02)

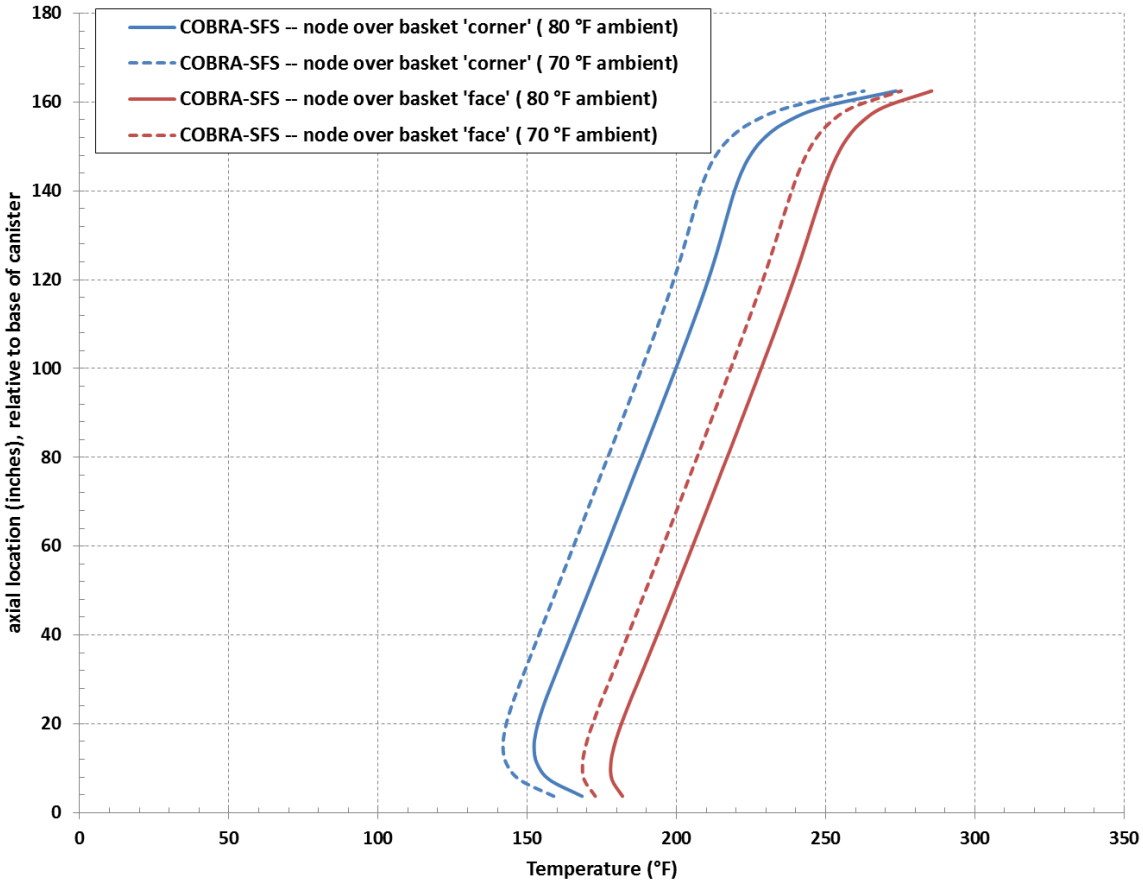

Figure 3-2. Axial Temperature Profiles on MPC Outer Shell: Module #516, MPC-170 (03-05)

The effect of the MPC-32 basket geometry on the circumferential temperature distribution at the canister surface is illustrated more clearly by the plots shown in Figures 3-3 and 3-4 for the two Diablo Canyon modules. These circumferential plots are for the 80°F (27°C) ambient air temperature boundary condition. The results obtained at 70°F (21°C) show the same pattern, at slightly cooler temperatures, as expected for the boundary condition difference.

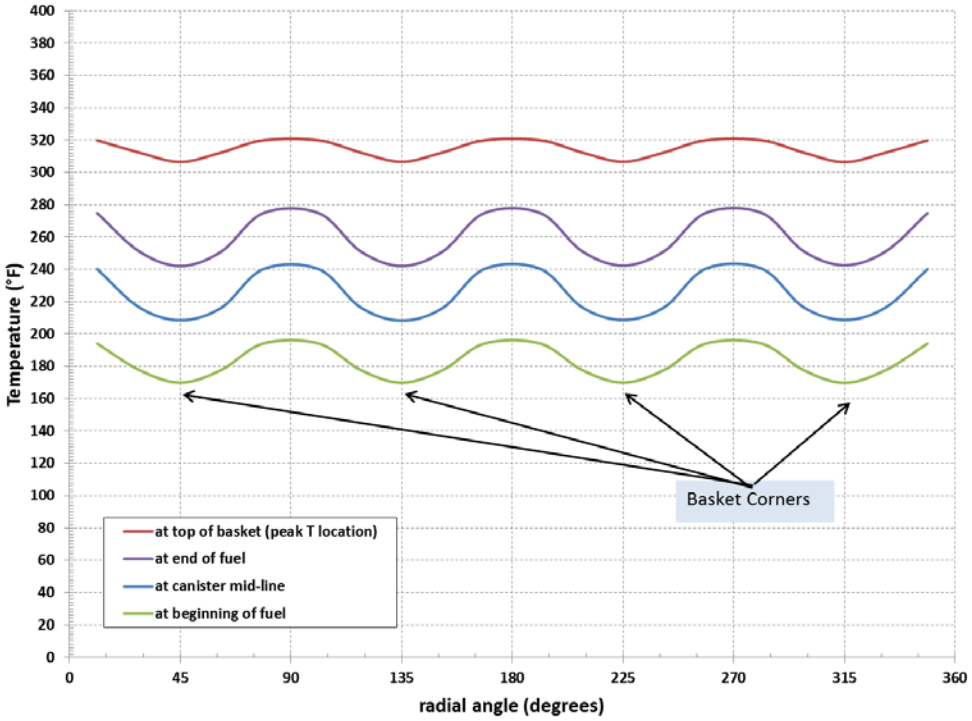

Figure 3-3. Circumferential Temperature Distributions on MPC Outer Shell: Module #318, MPC-123 (02-02), Ambient Air Temperature 80°F (27°C)

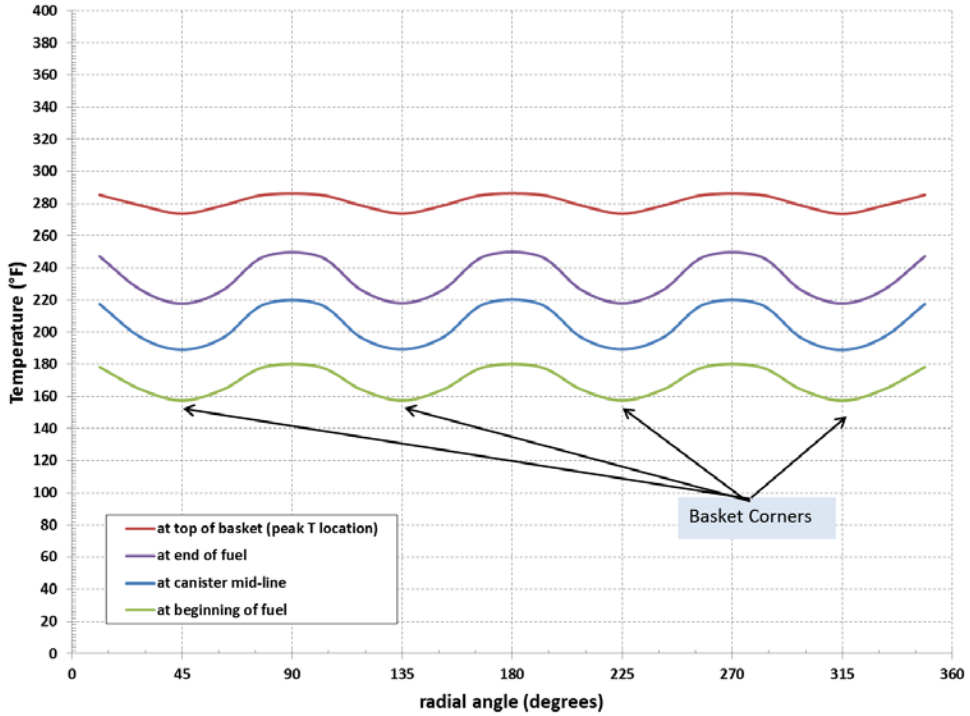

Figure 3-4. Circumferential Temperature Distributions on MPC Outer Shell: Module #516, MPC-170 (03-05), Ambient Air Temperature (80°F (27°C)

4.0 COMPARISON OF THERMAL MODELING TEMPERATURE PREDICTIONS TO MEASURED TEMPERATURES

The site inspection of MPC-123 and MPC-170 at the Diablo Canyon ISFSI was carried out over a 3-day period, January 14-16, 2014. The data obtained in the inspection is documented by Holtec (Holtec Int. 2014). This report is highly similar to the report on the Hope Creek inspection, containing the same background information and has similar omissions and deficiencies related to first time gathering of this type of data. It is therefore problematic to make quantitative assessment of measurement uncertainty, or reasonable estimates of sensitivity of surface temperatures to wind conditions. This section attempts to draw a qualitative assessment from the limited data set presented in the Holtec report.

Additional information to supplement some of the gaps in the Holtec report has been supplied by anecdotal reports from Used Fuel Disposition Campaign (UFDC) team members present on-site at the time of the inspection. No information about on-site weather conditions at the time of the inspection is available, other than the ambient air temperatures reported in conjunction with the measured surface temperatures. No information is provided on wind velocities at the site, but on-site observers report that the wind was quite calm throughout the three days of the inspection. Based on the limited data in the Holtec report, and anecdotal evidence supplied by on-site observers, the general sequence of events and conditions of the inspection are summarized in Table 4-1.

Table 4-1. Sequence of Events and Conditions of the Site Inspection at the Diablo Canyon ISFSI, January 14-16, 2014

Date	Module inspected	Inferred sequence of measurements	Weather summary
1/14/2014	MPC-170	TWO surface measurements taken on top lid of MPC; insertion depths of 64.5 in. and 7 in. NOTE: time not recorded, but timeframe of these measurements is estimated to have been around 1:30pm	ambient temperature recorded as 80°F (26.5°C)
1/15/2014	MPC-170	NINE surface measurements taken on side of MPC-170; insertion depths of 11 ft, 10.5 ft, 9.5 ft, 7.5 ft, and 3 ft down the annulus NOTE: time not recorded, but estimated from about 10:00AM to 1:30PM, from first to last measurement	ambient air temperature recorded as 70°F to 76°F (21 to 24.6°C)
	MPC-123	TWO temperature measurements taken on the top lid of the MPC-123; insertion depths of 64.5 inches and 7 inches NOTE: time not recorded, but timeframe of these measurements is estimated to have been around 4:00pm	ambient air temperature recorded as 68°F(20°C) and 70°F (21°C)
1/16/2014	MPC-123	NINE surface temperature measurements taken on side of MPC; insertion depths of 14 ft, 11.5 ft, 11 ft, 10.5 ft, 7.5 ft, and 3 ft down the annulus NOTE: measurement times not recorded, but estimated from about 10:00AM to 4:00PM, from first to last measurement	ambient air temperature ranged from 67°F (19.4°C) to 78°F (25.6°C)

For simplicity, it is assumed that the reported ambient air temperature and surface temperature measurements were taken at times close to the time of sampling (in the cases where the time of sampling can be estimated.) The specific surface temperature and ambient air temperature measurements obtained in the inspection are presented in Section 4.1, for each day of the inspection. In the discussion of measurement times in these sections, it is assumed that the timeframe of activities on any given day spanned a typical "day shift" from 9:00AM to 5:00PM. This is based on the stated time limit of 7 hours in the documented Holtec procedure (Holtec Int. 2014) for the inspection, defining the maximum time the inspection tool and hardware would be allowed to obstruct the outlet vent.

4.1 Summary of Temperature Measurements Obtained During Diablo Canyon Site Inspection

During the three days of the site inspection at the Diablo Canyon ISFSI, a total of 22 surface temperature measurements were obtained on the two canisters (MPC-123 and MPC-170). These temperature measurements were obtained in conjunction with dry and wet sampling of the surfaces with the Holtec-designed sampling tool. The sampling measurements are reported elsewhere, and are of no relevance to the thermal analysis. This report deals with the temperature measurements only. Table 4-2 summarizes the measured temperatures reported by Holtec (Holtec Int., 2014) for the side surface and top lid surface of MPC-170. Table 4-3 summarizes the measured temperatures reported for the side surface and top lid surface of MPC-123.

Table 4-2. Site Inspection Results: Temperature Measurements on MPC-170

Date	Estimated time (assume PST; 24-hr clock)	(Arbitrary) data number	Insertion depth (ft)	Measured top lid surface temperature (°F)	Measured side surface temperature (°F)	(Measured) ambient air temperature (°F)
1/14/2014	13:30	1	5.4	187.6		79.8
	13:30	2	0.6	190.4		79.7
1/15/2014	10:00	1	11		153.9	71.2
	10:15	2	7.5		193.8	69.5
	10:30	3	3		180.6	71.8
	11:00	4	10.5		177.5	70.7
	11:08	5	10.5		176.1	70.7
	13:00	6	9.5		182.8	72.1
	13:08	7	9.5		179.7	72.1
	13:30	8	9		188.2	76.3
	13:38	9	9		186.1	76.3

Table 4-3. Site Inspection Results: Temperature Measurements on MPC-123

Date	Estimated time (assume PST; 24-hr clock)	(Arbitrary) data number	Insertion depth (ft)	Measured top lid surface temperature (°F)	Measured side surface temperature (°F)	(Measured) ambient air temperature (°F)
1/15/2014	15:00	1	5.4	206.8		68.3
	15:15	2	0.6	204		69.9
1/16/2014	14:00	1	11		177.2	72.2

	14:20	2	7.5		211.7	77.1
	14:40	3	3		245.5	78.1
	10:00	4	14		119.7	66.9
	10:08	5	14		121.7	66.9
	11:00	6	11.5		173.4	66.9
	11:08	7	11.5		170.4	66.9
	11:30	8	10.5		187	73.3
	11:38	9	10.5		182	73.3

4.2 Comparison of Measured to Predicted Temperatures for MPC-170

This section presents a direct comparison of temperature predictions from the thermal modeling with COBRA-SFS to the measured temperatures obtained on the side surface and top lid surface of MPC-170 in the site inspection at the Diablo Canyon ISFSI. As shown in Figure 4-1, the ambient air temperature during the time of the inspection of MPC-170 ranged from 70°F to 80°F. Therefore, two sets of model predictions were obtained (see Section 3) for these bounding ambient air temperatures. The range of ambient air temperature variation shown in Figure 4-1 suggests relatively stable air temperature during the morning hours, and a fairly rapid increase in air temperature in the afternoon. The thermal modeling makes no attempt to predict the transient response of the system to this change. Transient evaluations are beyond the scope of this study, and there is insufficient information on changing boundary conditions to make this a worthwhile endeavor. The thermal modeling results presented here assume steady-state conditions, at the noted ambient air temperature.

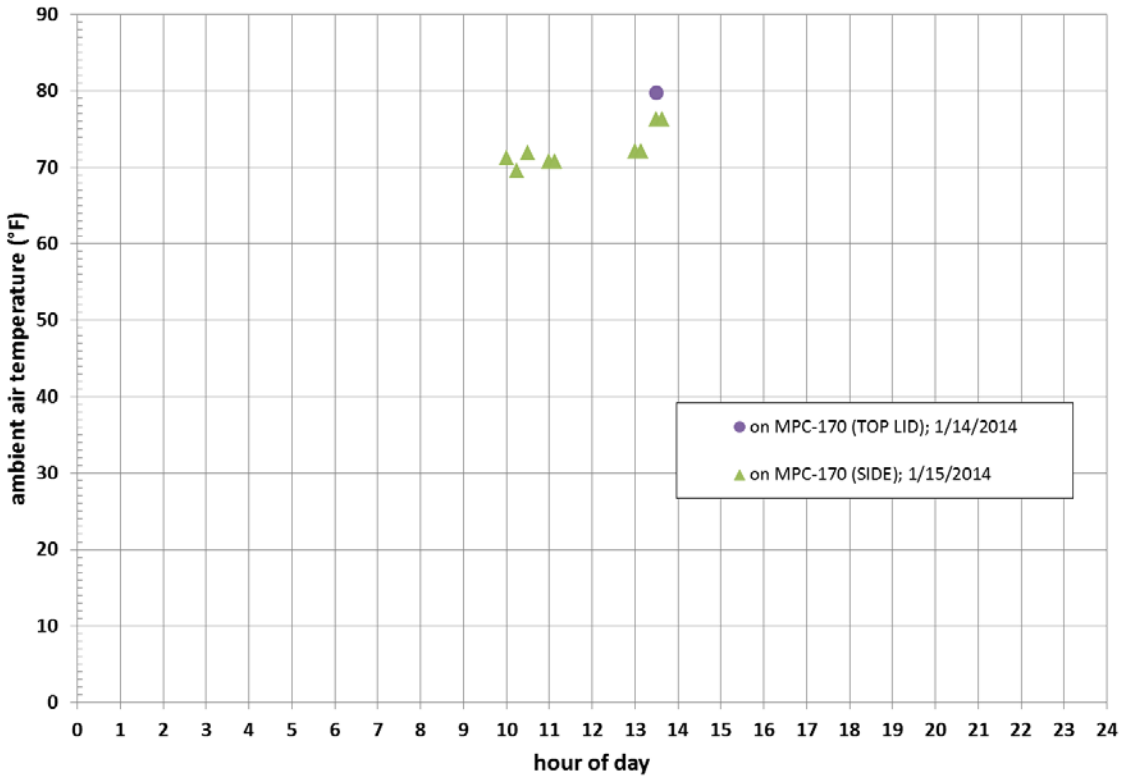

Figure 4-1. Ambient Air Temperatures Measured at in Conjunction with Surface Temperature Measurements on MPC-170

The temperatures measured on the side surface of MPC-170 were obtained on 1/15/2014, the second day of the site inspection. The insertion depths of the measurement tool down the annulus in these nine measurements ranged from 3 ft to 11 ft. Figure 4-2 shows a point-by-point plot of the measured temperatures compared to canister surface temperatures predicted with the COBRA-SFS thermal model. As discussed in Section 3, the geometry of the basket results in a significant circumferential variation in canister surface temperature (see Section 3, Figure 3-4). The indexing of the canister within the module overpack is not tracked in any way, so it is not possible to determine the circumferential position of the measured temperature relative to the geometry of the basket within the canister. Therefore, the comparison shows the maximum predicted temperature at a given axial location (over the face of the basket, shown as solid purple triangles on the graph), and the minimum predicted temperature (over the corner of the basket, shown as open purple triangles on the graph), in comparison to the measured temperature at a given axial location. Figure 4-3 shows the same comparison, with the measured data imposed on complete axial profiles of the predicted surface temperatures obtained in the thermal modeling.

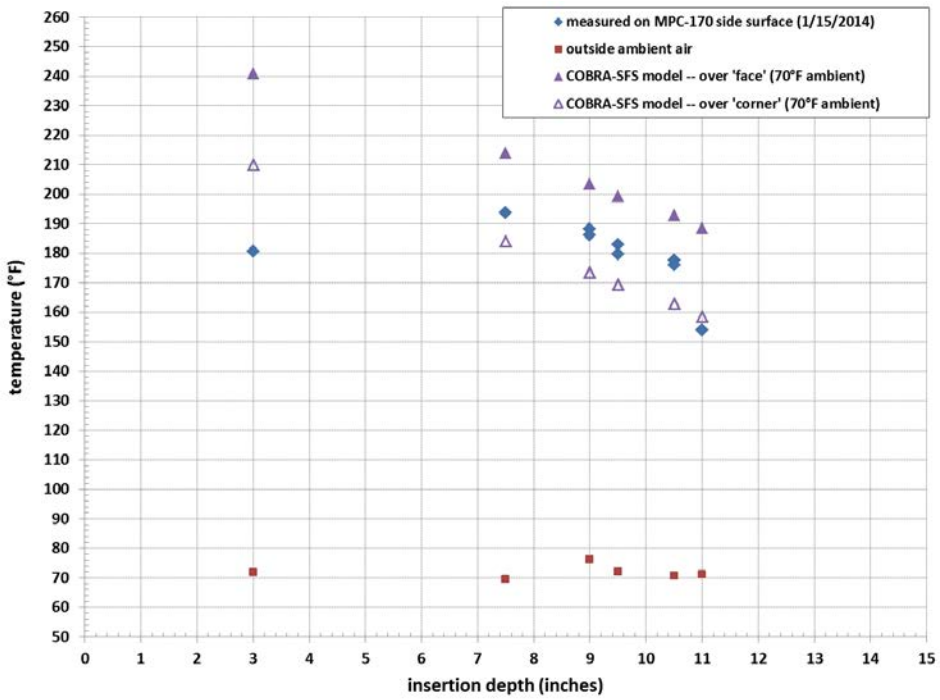

Figure 4-2. Point-by-Point Comparison of Thermal Modeling Results (at 70°F Ambient) to Measured Side Surface Temperatures on MPC-170

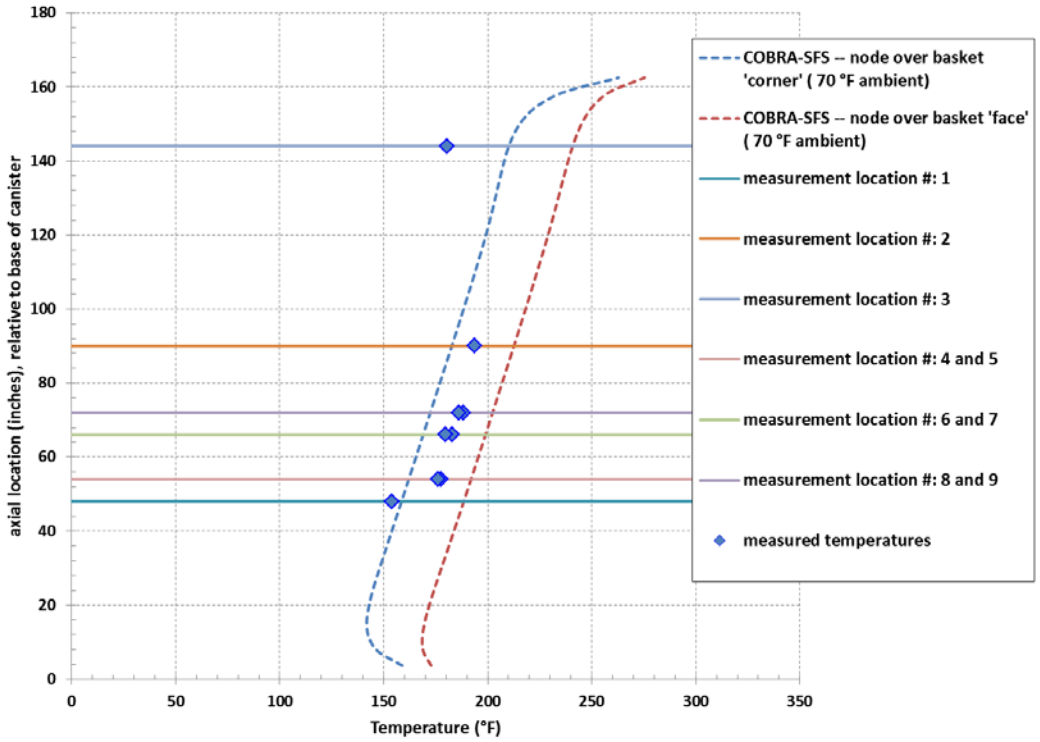

Figure 4-3. Comparison of Axial Profiles from Thermal Modeling Results (at 70°F Ambient) to Measured Side Surface Temperatures on MPC-170

The results in these two figures show that all but two of the measured temperatures fall very neatly between the maximum and minimum values predicted with the thermal model for a given axial location. Since the circumferential location is not known for the measured temperatures, this is as close as the comparison can come to full agreement between measured data and predictions. However, the measured temperatures also show two interesting anomalies, relative to axial location, that are not reflected in the model predictions. The measurements at 3 ft and at 11 ft are surprisingly low, relative to the measurements at the intermediate insertion depths, and in relation to the predicted profiles from the thermal modeling.

It is possible that these low measurements are due to incomplete contact between the side surface and the measurement instrument at these particular insertion depths, and these apparent outliers are simply bad data. However, there is no means of assessing the measurement uncertainty for any of this data, and based on what little is known about the measurement procedures, it is reasonable to assume that all of the measured data points on the canister side surface have essentially the same uncertainty. So there is no justification for rejecting these two points as bad data, while accepting the remaining seven as good data, simply because the former do not conform as nicely as the latter to the thermal modeling results.

The agreement between the modeling results and the measured temperatures in the more central axial locations suggest that the thermal model is appropriately capturing the complex thermal behavior of the MPC and the storage module. This includes heat transfer by conduction and thermal radiation within the fuel assemblies and canister, plus the hydrodynamics of the natural convection thermo-siphon through the basket and support rails within the canister, and

convection in the annulus between the canister and overpack. The fact that the two outlier data points are near the ends of the canister suggests that perhaps the axial distribution of decay heat within the canister is not adequately captured in the thermal model. This is the most reasonable explanation, based on available information, since the axial distribution in the model is a generic bounding profile (see Figure 2-11), rather than being based on measured axial burnup profiles for the fuel stored in this MPC.

No information has been provided on the actual axial decay heat for the fuel stored in MPC-170. The generic profile used in the model is probably a reasonable representation over most of the active fuel length, but is most likely to differ from reality near the ends of the active fuel length. Lacking information on the actual decay heat profile for the fuel in MPC-170, this suggestion is somewhat speculative, but it is a reasonable explanation for why the model agrees well with the data in one region, but not in another, where the heat transfer mechanisms are essentially the same, and there is no significant change in the geometry of the system.

Temperature measurements were obtained on the top lid surface of MPC-170 only at two locations, and only at locations near the outer rim of the canister lid. This is not sufficient information to produce a meaningful comparison to COBRA-SFS model predictions in this region, since the model uses a relatively simple 1-D representation of the canister and overpack lid region (as illustrated in Figure 2.1). Therefore, the top lid surface measurements have been omitted from the comparisons with model results.

4.3 Comparison of Measured to Predicted Temperatures for MPC-123

This section presents a direct comparison of temperature predictions from the thermal modeling with COBRA-SFS to the measured temperatures obtained on the side surface and top lid surface of MPC-123 in the site inspection at the Diablo Canyon ISFSI. As shown in Figure 4-4, the ambient air temperature during the time of the inspection of MPC-123 ranged from 68°F to 78°F. As with the evaluations for MPC-170, two sets of model predictions were obtained (see Section 3) with assumed ambient air temperatures of 70°F and 80°F, to reasonably bound the actual ambient conditions at the site.

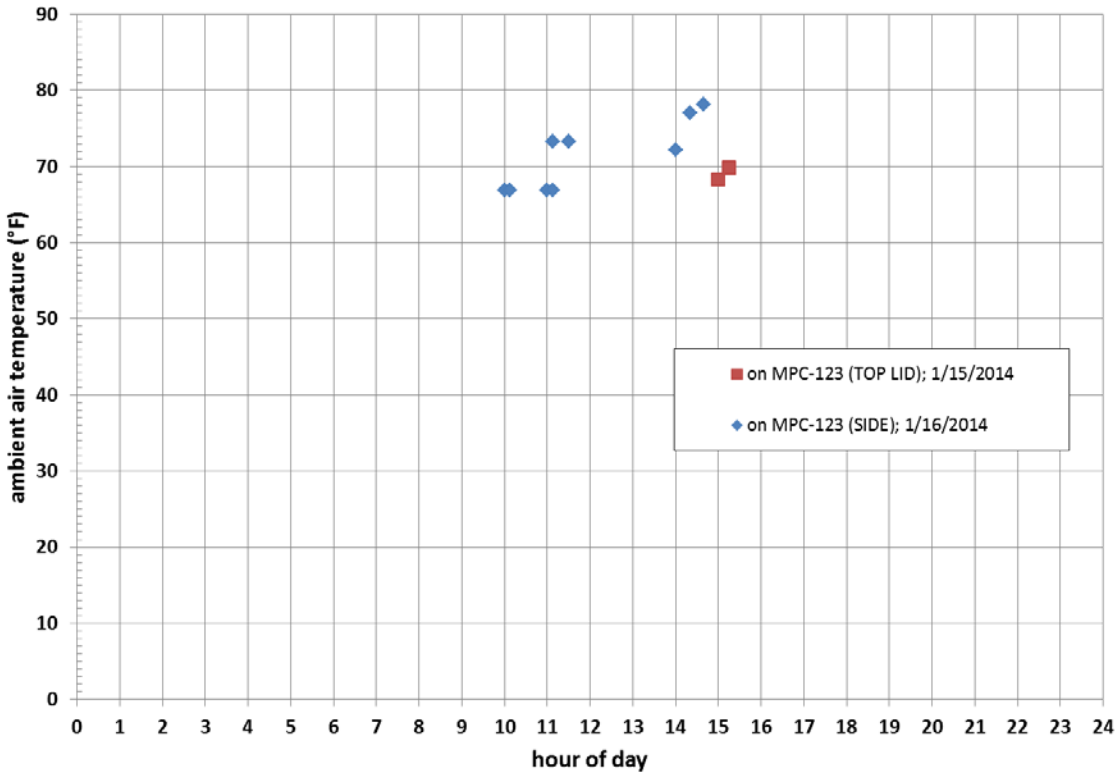

Figure 4-4. Ambient Air Temperatures Measured in Conjunction with Surface Temperature Measurements on MPC-123

The range of ambient air temperature variation shown in Figure 4-4 suggests the estimated timeframe for the measurements on 1/16/2014 is only approximate, as the gradient over the inspection time interval is not typical of a normal diurnal cycle. The thermal modeling makes no attempt to predict the transient response of the system to the apparently rapid change in ambient air temperature indicated by the time-scale in Figure 4-4. This time history is probably an artifact of incomplete reporting, and is not likely to be representative of the actual rate of change in ambient temperature during this day of the inspection. Transient evaluations are beyond the scope of this study, and there is insufficient information on changing boundary conditions to make this a worthwhile endeavor. The thermal modeling results presented here assume steady-state conditions, at a given ambient air temperature.

The temperatures measured on the side surface of MPC-123 were obtained on 1/16/2014, the third day of the site inspection. The insertion depths of the measurement tool down the annulus in these nine measurements ranged from 3 ft to 14 ft. As with MPC-170, no information is available on the indexing of the canister with respect to the overpack, so it is not possible to determine the circumferential location of the measurements on the MPC side surface, relative to the orientation of the basket. However, Figure 4-5 shows the measured data compared to the maximum and minimum predicted axial profiles (over the basket face and corner, respectively, as discussed in Section 3). This comparison suggests that the axial locations of the measured temperatures may have coincided with a basket corner.

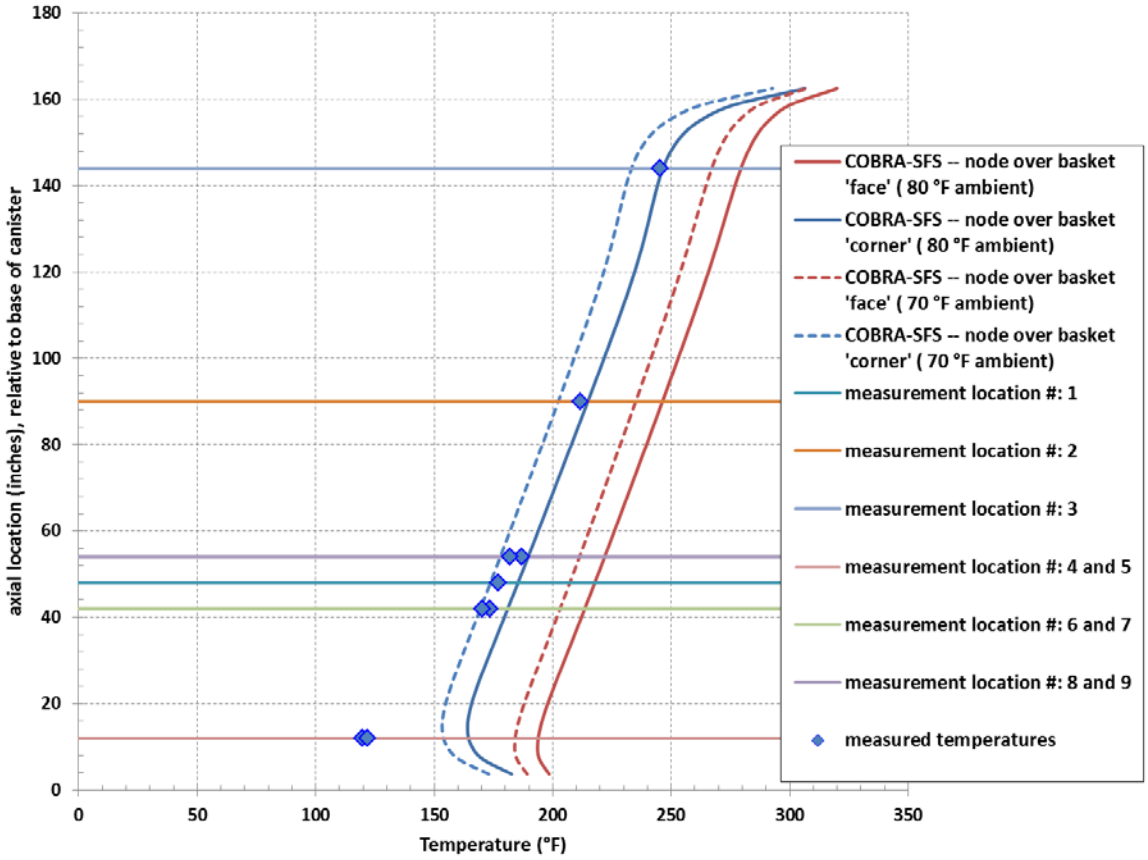

Figure 4-5. Comparison of Axial Profiles from Thermal Modeling Results (at 70°F Ambient and 80°F Ambient) to Measured Side Surface Temperatures on MPC-123

The comparison in Figure 4-5 shows that the predicted temperature profiles match the measured side surface temperatures quite well, within the variation of the measured ambient air temperature. This is more clearly illustrated in Figure 4-6, which shows a point-by-point plot of the measured temperatures compared to canister surface temperatures predicted with the COBRA-SFS thermal model. The plots in Figures 4-5 and 4-6 show consistent agreement between the measured data and the thermal model predictions, except at the 14-ft insertion depth. As discussed above, with similar results for the comparisons shown for MPC-170, this suggests that the axial decay heat profile assumed in the model may not be the same as that of the actual fuel within the canister.

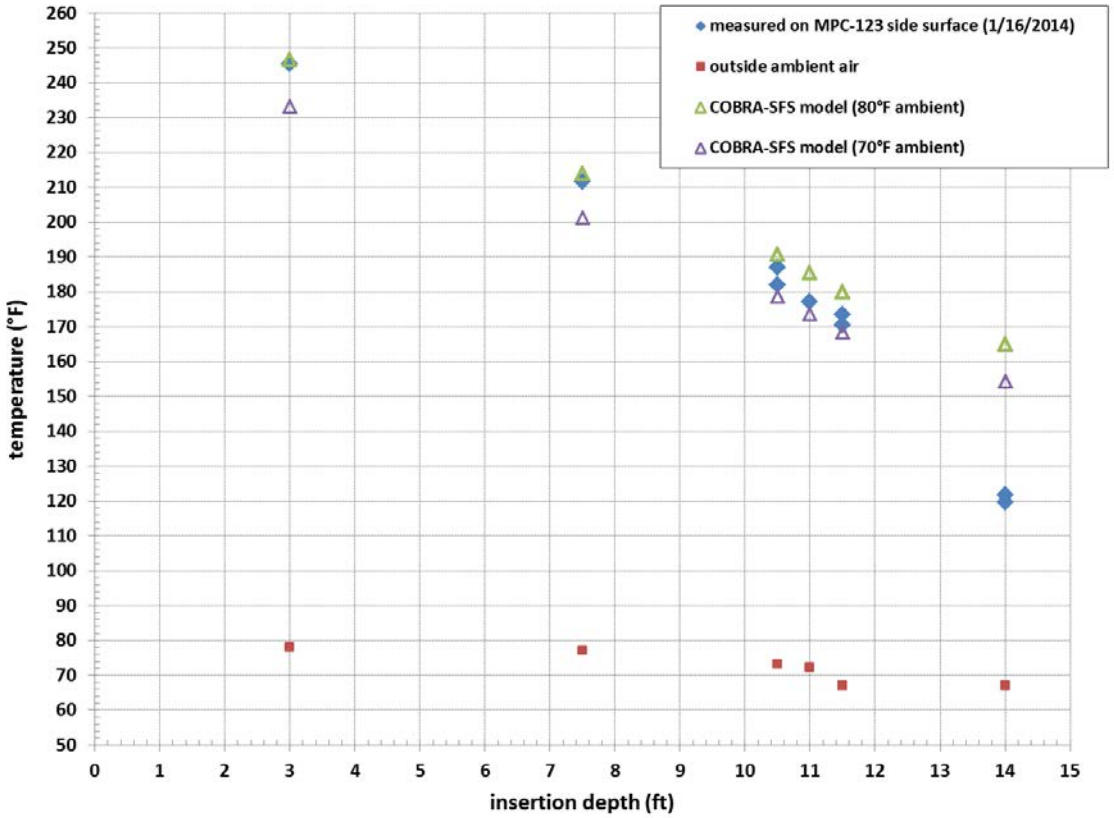

Figure 4-6. Point-by-Point Comparison of Thermal Modeling Results (at 70°F Ambient and 80°F Ambient) to Measured Side Surface Temperatures on MPC-123

Temperature measurements were obtained on the top lid surface of MPC-123 only at two locations, and only at locations near the outer rim of the canister lid. As noted at the end of Section 4.2 in the discussion of the top lid temperature measurements for MPC-170, this is not sufficient information to produce a meaningful comparison to COBRA-SFS model predictions in this region, since the model uses a relatively simple 1-D representation of the canister and overpack lid region. Therefore, the top lid surface measurements have been omitted from the comparisons with model results for the MPC-123, as well.

5.0 CONCLUSIONS

The post-inspection comparison of modeling results to measured data from the Diablo Canyon site inspection shows that thermal modeling with the COBRA-SFS code can yield reasonable estimates of temperatures and temperature distributions in an actual storage module within an operating ISFSI. The assumption of steady-state conditions with still air can yield good agreement with measured temperatures, if the assumption is a reasonable approximation of actual conditions. The more uniform daytime temperatures and calm wind at Diablo Canyon, in comparison to non-equilibrium conditions that prevailed at the Hope Creek ISFSI, show the importance of ambient conditions for obtaining representative data that can be usefully compared to results from steady-state models.

Differences in measured temperatures compared to model predictions near the ends of the canister suggest the importance of accurate characterization of the axial distribution of decay heat for the fuel stored in the canister. Based on the comparison with the inspection data obtained at the Diablo Canyon ISFSI, uncertainty in this modeling parameter may lead to significant uncertainty in predictions of temperatures near the ends of the canister.

The usefulness of thermal evaluations for a specific site depend on the accuracy of the model that can be constructed for the site being inspected. This means having timely access to information on the storage module configuration, the configuration and condition of the fuel stored within the canisters to be inspected, and some reasonable expectation that ambient conditions at the time of the inspection will be consistent with modeling assumptions of steady-state conditions with still air. In addition, complete information on overall boundary conditions would be helpful. Specifically,

- Accurate information on assembly total decay heat, or information quantifying the nominal conservatism in assembly decay heat values developed by the utility for operational and licensing compliance, would be helpful in obtaining meaningful comparisons between predicted and measured temperatures.
- Accurate information on assembly axial decay heat profiles (in general corresponding to axial burnup profiles) is needed to fully characterize the axial distribution of temperature on the storage canister outer shell.
    - This information seems generally unavailable at operating ISFSIs, so an alternative approach could be to perform modeling studies to quantify the uncertainty in surface temperatures (and internal component temperatures) due to variation in assumed axial decay heat profiles, relative to realistic profiles, for a range of fuel types.
- Accurate information on site-specific variations from the nominal design basis of the storage module or canister is needed to be able to predict accurate detailed temperature distributions, particularly on surfaces that might potentially be accessible for on-site inspection and measurement.

6.0 REFERENCES

10 CFR 71. 2003. "Packaging and Transportation of Radioactive Material." C*ode of Federal Regulations,* U.S. Nuclear Regulatory Commission, Washington D.C.

Creer JM, TE Michener, MA McKinnon, JE Tanner, ER Gilbert, and RL Goodman. 1987. *The TN-24P PWR Spent-Fuel Storage Cask: Testing and Analysis*. EPRI-NP-5128/PNL-6054, Electric Power Research Institute, Palo Alto, California.

Cuta JM and HE Adkins. 2013. *Preliminary Thermal Modeling of HI-STORM100S-218 Version B Storage Modules at Hope Creek Nuclear Power Station ISFSI.* FCRD-UFD-2013-000297, PNNL-22552. U.S. Department of Energy, Used Fuel Disposition Campaign, Washington, D.C.

Cuta JM and HE Adkins. 2014. *Preliminary Thermal Modeling of HI-STORM100 Storage Modules at Diablo Canyon Power Plant ISFSI.* FCRD-UFD-2014-000505, PNNL-23298. U.S. Department of Energy, Used Fuel Disposition Campaign, Washington, D.C.

Cuta JM and HE Adkins. 2015. *Post-Inspection Evaluation: Thermal Modeling of HI-STORM100S-218 Version B Storage Modules at Hope Creek Nuclear Power Station ISFSI.* FCRD-UFD-2015-000491, PNNL-24542. U.S. Department of Energy, Used Fuel Disposition Campaign, Washington, D.C.

DOE. 1998. *Topical Report on Actinide-Only Burnup Credit for PWR Spent Nuclear Fuel Packages*. DOE/RW-0472, Revision 2, Office of Civilian Radioactive Waste Management, Washington D.C., U.S. Department of Energy.

Holtec International. 2010. *Final Safety Analysis Report for the HI-STORM 100 Cask System, Revision 9.* Holtec Report No. HI-2002444, USNRC Docket No. 72-1014. Holtec International, Marlton, NJ. February 13, 2010. NOTE: this document is copyrighted intellectual property of Holtec International. All rights reserved.

Holtec International (Company Private document). 2014. *MPC Surface Inspection at Diablo Canyon Power Plant.* for EPRI. Holtec Report No. HI-2146301, Holtec Project No. 920. Sponsoring Holtec Division: NPD. Report Class: Safety Related. Revision 0, approved December 8, 2014.

Lombardo NJ, JM Cuta, TE Michener, DR Rector, and CL Wheeler. 1986. *COBRA-SFS: A Thermal-Hydraulic Analysis Computer Code, Volume III: Validation Assessments*. PNL-6048 Vol. III. Pacific Northwest Laboratory, Richland, Washington.

Michener TE, DR Rector, JM Cuta, RE Dodge, and CW Enderlin. 1995. *COBRA-SFS: A Thermal-Hydraulic Code for Spent Fuel Storage and Transportation Casks*. PNL-10782, Pacific Northwest Laboratory, Richland, Washington.

NOAA 2013. " National Weather Service Forecast Office, Los Angeles/Oxnard." Data for San Luis Obispo, CA, accessed 11/12/2013 at http://www.wrh.noaa.gov/yeardisp.php?stn=KSBP&wfo=lox&year=2012&span=Calendar+Year

Peterson J, et al. 2013. *Used Nuclear Fuel Storage Transportation Disposal Analysis Resources and Data System (UNF-ST&DARDS).* FCRD-NFST-2013-000117 Rev. 0, Oak Ridge National Laboratory, Oak Ridge, Tennessee.

Rector DR, RA McCann, UP Jenquin, CM Heeb, JM Creer, and CL Wheeler. 1986. *CASTOR-1C Spent Fuel Storage Cask Decay Heat, Heat Transfer and Shielding Analysis*. PNL-5974. Pacific Northwest Laboratory, Richland, Washington.

Sparrow EM, and LFA Azevedo. 1985. "Vertical-channel natural convection spanning between the fully-developed limit and the single-plate boundary-layer limit." I*nternational Journal of Heat and Mass Transfer*, 28(10):1847-1857.

Sparrow EM, AL Loeffler, and HA Hubbard. 1961. "Heat Transfer to Longitudinal Laminar Flow between Cylinders." *Journal of Heat Transfer*, 83:415.

Suffield SR, JM Cuta, JA Fort, BA Collins, HE Adkins, and ER Siciliano. 2012. *Thermal Modeling of NUHOMS HSM-15 and HSM-1 Storage Modules at Calvert Cliffs Nuclear Power Station ISFSI.* PNNL-21788, Pacific Northwest National Laboratory, Richland, Washington.

Appendix A

Post-Inspection Predictions of Axial Temperature Distribution on Canister Shell

Appendix A: Post-Inspection Predictions of Axial Temperature Distribution on Canister Shell

This appendix presents the axial temperature distributions on the MPC outer shell predicted with the COBRA-SFS model of modules #318 (02-02) and #516 (03-05) in the Diablo Canyon ISFSI. These profiles are through the location of the peak temperature on the MPC outer shell for each configuration. A second profile is provided for the peak temperature in the cooler regions opposite the MPC-32 basket corners, showing the circumferential variation in canister shell temperature predicted for this storage system. The axial location in the tables is relative to the inner surface of the canister base. Results are presented for MPC-123 in Tables A-1 and A-2, for ambient temperature of 70°F (21.1°C) and 80°F (26.7°F), respectively. Similarly, results for MPC-170 at these two ambient temperatures are presented in Tables A-3 and A-4. These tables present thermal evaluation results for ambient conditions approximating the range of ambient temperatures that were encountered when surface temperatures were measured during the inspection.

Table A-1. Canister Shell Axial Temperature Distributions: Module #318, MPC 123 (02-02) for Ambient Air Temperature of 70°F (21.1°C)

Ambient:	**70°F (21.1°C)**			
axial location	**peak profile**		**profile over basket corner**	
(inches)	**(°F)**	**(°C)**	**(°F)**	**(°C)**
3.7	189.20	87.3	172.99	78.3
7.4	184.67	84.8	159.65	70.9
11.1	184.00	84.4	154.47	68.0
14.8	185.10	85.1	153.32	67.4
18.5	187.02	86.1	154.15	67.9
22.2	189.33	87.4	155.96	68.9
25.9	191.83	88.8	158.23	70.1
29.5	194.40	90.2	160.72	71.5
33.2	196.98	91.7	163.30	72.9
36.9	199.57	93.1	165.91	74.4
40.6	202.13	94.5	168.52	75.8
44.3	204.68	95.9	171.11	77.3
48	207.21	97.3	173.70	78.7
51.7	209.72	98.7	176.27	80.1
55.4	212.21	100.1	178.82	81.6
59.1	214.68	101.5	181.36	83.0
62.8	217.14	102.9	183.89	84.4
66.5	219.59	104.2	186.40	85.8
70.2	222.03	105.6	188.91	87.2
73.9	224.46	106.9	191.42	88.6
77.6	226.88	108.3	193.92	90.0
81.2	229.30	109.6	196.41	91.3
84.9	231.71	110.9	198.90	92.7

88.6	234.11	112.3	201.38	94.1
92.3	236.50	113.6	203.86	95.5
96	238.89	114.9	206.33	96.9
99.7	241.26	116.3	208.79	98.2
103.4	243.62	117.6	211.22	99.6
107.1	245.97	118.9	213.63	100.9
110.8	248.28	120.2	215.99	102.2
114.5	250.56	121.4	218.29	103.5
118.2	252.79	122.7	220.48	104.7
121.9	254.94	123.9	222.55	105.9
125.6	257.00	125.0	224.46	106.9
129.3	258.99	126.1	226.20	107.9
133	260.91	127.2	227.80	108.8
136.6	262.82	128.2	229.37	109.7
140.3	264.82	129.3	231.08	110.6
144	267.06	130.6	233.22	111.8
147.7	269.74	132.1	236.21	113.4
151.4	273.25	134.0	240.83	116.0
155.1	278.50	136.9	248.74	120.4
158.8	287.69	142.1	263.47	128.6
162.5	306.76	152.6	292.73	144.9

Table A-2. Canister Shell Axial Temperature Distribution: Module #318, MPC 123 (02-02) for Ambient Air Temperature of 80°F (21.1°C)

Ambient:	**80°F (26.7°C)**			
axial location	**peak profile**		**profile over basket corner**	
(inches)	**(°F)**	**(°C)**	**(°F)**	**(°C)**
3.7	198.46	92.5	182.67	83.7
7.4	194.19	90.1	169.85	76.6
11.1	193.69	89.8	164.99	73.9
14.8	194.91	90.5	164.04	73.4
18.5	196.93	91.6	165.03	73.9
22.2	199.33	93.0	166.97	75.0
25.9	201.91	94.4	169.35	76.3
29.5	204.56	95.9	171.94	77.7
33.2	207.22	97.3	174.61	79.2
36.9	209.87	98.8	177.30	80.7
40.6	212.51	100.3	179.99	82.2
44.3	215.13	101.7	182.67	83.7
48	217.72	103.2	185.33	85.2
51.7	220.30	104.6	187.98	86.7
55.4	222.86	106.0	190.61	88.1
59.1	225.40	107.4	193.22	89.6
62.8	227.93	108.8	195.82	91.0

66.5	230.44	110.2	198.41	92.4
70.2	232.95	111.6	200.99	93.9
73.9	235.44	113.0	203.57	95.3
77.6	237.93	114.4	206.14	96.7
81.2	240.41	115.8	208.71	98.2
84.9	242.89	117.2	211.27	99.6
88.6	245.36	118.5	213.83	101.0
92.3	247.82	119.9	216.38	102.4
96	250.27	121.3	218.92	103.8
99.7	252.72	122.6	221.45	105.3
103.4	255.15	124.0	223.96	106.6
107.1	257.57	125.3	226.44	108.0
110.8	259.95	126.6	228.87	109.4
114.5	262.30	127.9	231.23	110.7
118.2	264.60	129.2	233.49	111.9
121.9	266.82	130.5	235.61	113.1
125.6	268.95	131.6	237.57	114.2
129.3	271.01	132.8	239.34	115.2
133	272.99	133.9	240.98	116.1
136.6	274.98	135.0	242.58	117.0
140.3	277.06	136.1	244.32	118.0
144	279.39	137.4	246.51	119.2
147.7	282.16	139.0	249.54	120.9
151.4	285.78	141.0	254.22	123.5
155.1	291.15	144.0	262.18	127.9
158.8	300.51	149.2	276.99	136.1
162.5	319.92	160.0	306.41	152.4

Table A-3. Canister Shell Axial Temperature Distribution: Module #516, MPC 170 (03-05) for Ambient Air Temperature of 70°F (21.1°C)

Ambient:	**70°F (21.1°C)**			
axial location	**peak profile**		**profile over basket corner**	
(inches)	**(°F)**	**(°C)**	**(°F)**	**(°C)**
3.7	172.80	78.2	105.87	41.04
7.4	169.06	76.1	94.01	34.45
11.1	168.53	75.9	90.08	32.27
14.8	169.47	76.4	89.46	31.92
18.5	171.11	77.3	90.21	32.34
22.2	173.09	78.4	91.55	33.08
25.9	175.23	79.6	93.12	33.95
29.5	177.43	80.8	94.79	34.88
33.2	179.65	82.0	96.50	35.83
36.9	181.87	83.3	98.22	36.79

40.6	184.08	84.5	99.96	37.75
44.3	186.28	85.7	101.69	38.72
48	188.46	86.9	103.42	39.68
51.7	190.62	88.1	105.16	40.64
55.4	192.77	89.3	106.89	41.61
59.1	194.91	90.5	108.63	42.57
62.8	197.04	91.7	110.38	43.54
66.5	199.16	92.9	112.13	44.51
70.2	201.28	94.0	113.88	45.49
73.9	203.38	95.2	115.65	46.47
77.6	205.49	96.4	117.42	47.45
81.2	207.58	97.5	119.20	48.44
84.9	209.67	98.7	120.99	49.44
88.6	211.76	99.9	122.79	50.44
92.3	213.84	101.0	124.60	51.44
96	215.92	102.2	126.42	52.45
99.7	217.99	103.3	128.24	53.47
103.4	220.05	104.5	130.07	54.48
107.1	222.09	105.6	131.90	55.50
110.8	224.11	106.7	133.72	56.51
114.5	226.10	107.8	135.52	57.51
118.2	228.05	108.9	137.29	58.49
121.9	229.94	110.0	139.00	59.45
125.6	231.76	111.0	140.65	60.36
129.3	233.52	112.0	142.21	61.23
133	235.24	112.9	143.71	62.06
136.6	236.96	113.9	145.18	62.88
140.3	238.77	114.9	146.70	63.72
144	240.79	116.0	148.38	64.66
147.7	243.20	117.3	150.39	65.77
151.4	246.34	119.1	153.09	67.27
155.1	250.98	121.7	157.35	69.64
158.8	259.00	126.1	165.44	74.13
162.5	275.31	135.2	183.02	83.90

Table A-4. Canister Shell Axial Temperature Distribution: Module #516, MPC 170 (03-05) for Ambient Air Temperature of 80°F (26.7°C)

Ambient:	**80°F (26.7°C)**			
axial location	**peak profile**		**profile over basket corner**	
(inches)	**(°F)**	**(°C)**	**(°F)**	**(°C)**
3.7	181.90	83.3	168.37	75.8
7.4	178.40	81.3	157.47	69.7
11.1	178.00	81.1	153.22	67.3

14.8	179.02	81.7	152.28	66.8
18.5	180.72	82.6	152.98	67.2
22.2	182.75	83.7	154.49	68.1
25.9	184.92	85.0	156.40	69.1
29.5	187.16	86.2	158.50	70.3
33.2	189.41	87.5	160.67	71.5
36.9	191.67	88.7	162.88	72.7
40.6	193.90	89.9	165.09	73.9
44.3	196.13	91.2	167.29	75.2
48	198.34	92.4	169.49	76.4
51.7	200.53	93.6	171.67	77.6
55.4	202.71	94.8	173.85	78.8
59.1	204.87	96.0	176.02	80.0
62.8	207.03	97.2	178.18	81.2
66.5	209.17	98.4	180.34	82.4
70.2	211.31	99.6	182.49	83.6
73.9	213.44	100.8	184.64	84.8
77.6	215.56	102.0	186.79	86.0
81.2	217.68	103.2	188.93	87.2
84.9	219.80	104.3	191.07	88.4
88.6	221.90	105.5	193.21	89.6
92.3	224.01	106.7	195.35	90.7
96	226.11	107.8	197.48	91.9
99.7	228.20	109.0	199.60	93.1
103.4	230.27	110.2	201.71	94.3
107.1	232.34	111.3	203.79	95.4
110.8	234.38	112.4	205.84	96.6
114.5	236.39	113.5	207.83	97.7
118.2	238.35	114.6	209.75	98.8
121.9	240.26	115.7	211.58	99.8
125.6	242.10	116.7	213.29	100.7
129.3	243.87	117.7	214.88	101.6
133	245.60	118.7	216.40	102.4
136.6	247.34	119.6	217.92	103.3
140.3	249.16	120.6	219.58	104.2
144	251.19	121.8	221.64	105.4
147.7	253.61	123.1	224.44	106.9
151.4	256.75	124.9	228.66	109.3
155.1	261.38	127.4	235.73	113.2
158.8	269.34	131.9	248.60	120.3
162.5	285.53	140.8	273.59	134.2